LIBRARY OF THE
UNIVERSITY OF ILLINOIS
AT URBANA-CHAMPAIGN
510.84
Il6r
no.111-130
cop.3

The person charging this material is responsible for its return to the library from which it was withdrawn on or before the **Latest Date** stamped below.

Theft, mutilation, and underlining of baaks are reasans for disciplinary actian and may result in dismissal from the University.

To renew call Telephane Center, 333-8400

UNIVERSITY OF ILLINOIS LIBRARY AT URBANA-CHAMPAIGN

BUILDING USE ONLY

SEP 21 1980

SEP 29 1980

L161—O-1096

Digitized by the Internet Archive
in 2013

http://archive.org/details/studyofsaturatio115ribe

510.84
I2Gr
no.115
cop. 3

UNIVERSITY OF ILLINOIS
GRADUATE COLLEGE
DIGITAL COMPUTER LABORATORY

REPORT NO. 115

A STUDY ON SATURATION PHENOMENA

by
Sergio T. Ribeiro

April 9, 1962

This work was supported in part by the Office of
Naval Research under Contract Nonr-1834(15).

UNIVERSITY OF ILLINOIS
GRADUATE COLLEGE
DIGITAL COMPUTER LABORATORY

REPORT NO. 115

A STUDY ON SATURATION PHENOMENA

by

Sergio T. Ribeiro

April 9, 1962

This work was supported in part by the Office of Naval Research under Contract Nonr-1834(15).

TABLE OF CONTENTS

		Page
I.	SATURATION	1
	1. Introduction	1
	2. Measurement of Admittance Parameters	2
	3. Direct Measurements of r_B and $(r_B + r_C)$	5
	4. Comments	5
	5. Experimental Results	7
	a. General Remarks	7
	b. Tables of Data	8
	c. Graphs	17
	d. Empirical Formula for r_C	17
	6. Theoretical Analysis	24
	a. Time Independent Solution	24
	b. Time Dependent Diffusion Equation	26
	c. Solution of the Time Dependent Equation	27
	d. Periodic Boundary Conditions	28
	e. Admittance Parameters	30
	f. Equivalent Circuit Parameters	33
	g. Dependence of r_C and α on ρ_E and ρ_C	35
	h. Behavior of r_B and r_E	38
	i. Variations of L_p and τ_p	39
II.	SUPERSATURATION	44
	1. Introduction	44
	2. Attempted Explanation Neglecting the Early Effect	45
	3. Interpretation through the Early Effect	47
	4. Expanded Expression for G_I	49
	5. Qualitative Discussion of G_I	51
	6. Quantitative Example	53
	7. Influence of the Early Effect on the Measurement of Parameter Values	57

PART I

SATURATION

1. Introduction

The purpose of this report is to describe an investigation of junction transistor behavior under saturation conditions. It was not our purpose to obtain statistical data of any sort, but rather, to acquire some insight into the physical phenomena involved in saturation. Most important of all, we wished to find, even if in a qualitative way, the relative importance of the physical phenomena involved in saturation on the general degeneration of transistor properties.

With this purpose in mind, we decided to measure the small signal parameters of the equivalent circuit of Fig 1. as functions of I_E and V_C,

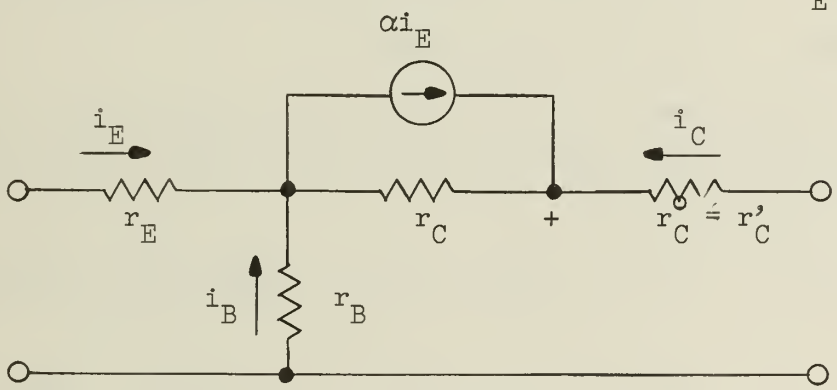

Figure 1. Equivalent Circuit

the biasing emitter current and collector voltage, because these are the parameters that best represent (in a first approximation) the physical properties of the transistor.

However, direct measurement of these parameters is not practical, so it was decided to measure the small signal admittance parameters directly and, from these, to compute the values of r_E, r_B, r_C' and α. For this purpose we constructed an instrument which will be presently described.

Our next objective was to calculate the theoretical values of these parameters as functions of I_E and V_C from standard junction transistor theory and check these theoretical results against experimental results. We arbitrarily selected mesa transistors of the type GF-45011 as samples for the experiment.

In measuring $y_{12} = \frac{i_E}{v_C}\Big|_{v_E = 0}$ and $y_{22} = \frac{i_C}{v_C}\Big|_{v_E = 0}$, we noticed that, much to our surprise, i_E was larger than i_C for certain values of I_E and V_C. This super-saturation effect of reverse current gain only occurs at high values of I_E (typically I_E = 50 ma) and low values of V_C (typically V_C = 0.5v), is very critical with respect to variations of I_E, V_C and temperature, and does not seem to occur for every kind of transistor; up to the moment we were only able to notice it in the GF-45011 and at different current and voltage levels, in the S-166.

2. Measurement of Admittance Parameters

The admittance parameters were chosen because, with the means at our disposal, we could better approximate AC short circuit conditions than AC open circuit conditions.

Since a series of measurements was needed, the instrument was to be practical, and still furnish an acceptable accuracy.

A short circuit condition can be approximated by means of a high gain amplifier with feed back, as illustrated in Fig. 2.

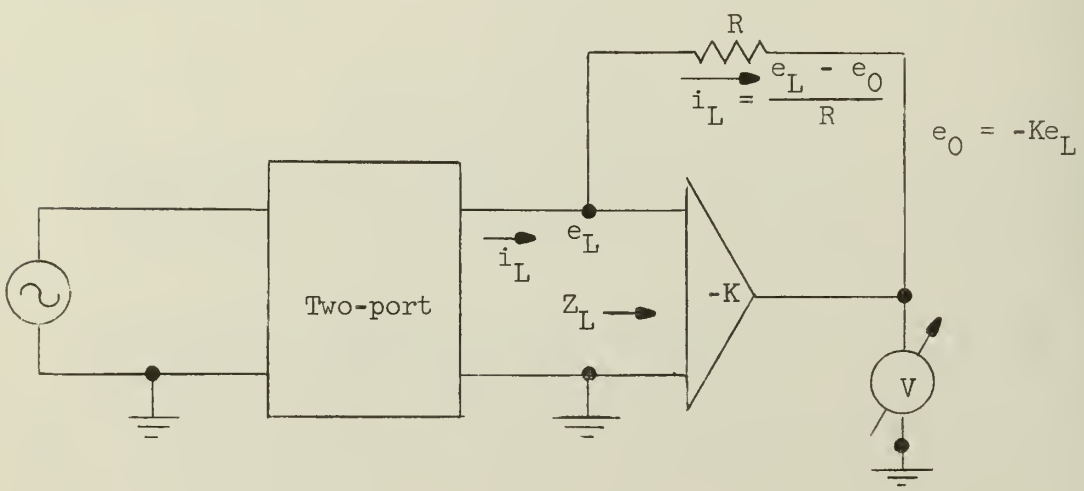

Figure 2. Measurement of Output Current

It is seen that $Z_L = \frac{e_L}{i_L} = \frac{e_L}{\frac{e_L - e_0}{R}} = R\,\frac{e_L}{(1+K)e_L}$, i.e.,

$$Z_L = \frac{R}{1+K} \tag{1}$$

So that, if K is positive and large we will have

$$Z_L \approx \frac{R}{K} \tag{2}$$

Furthermore,

$$e_0 = -KZ_L i_L, \text{ i.e.}$$

$$e_0 = -\frac{K}{K+1} R i_L \tag{3}$$

So that, if K is large,

$$e_0 \approx -Ri_L \tag{4}$$

This provides us with a means of measuring i_L in the case where e_L is very small by measuring e_0, and R, which can be selected once and for all.

A slight modification of this scheme allows us to measure input currents also, as is shown in Fig. 3.

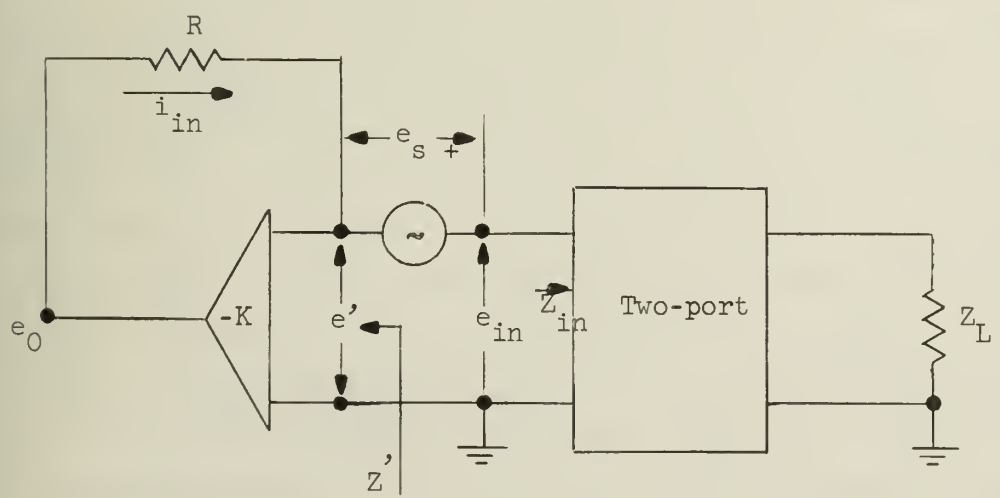

Figure 3. Measurement of Input Current

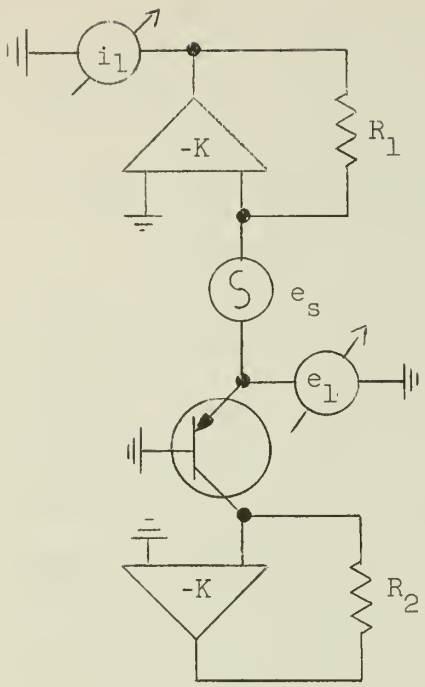

(a) Measurement of y_{11}

$$y_{11} = \frac{i_1}{e_1}$$

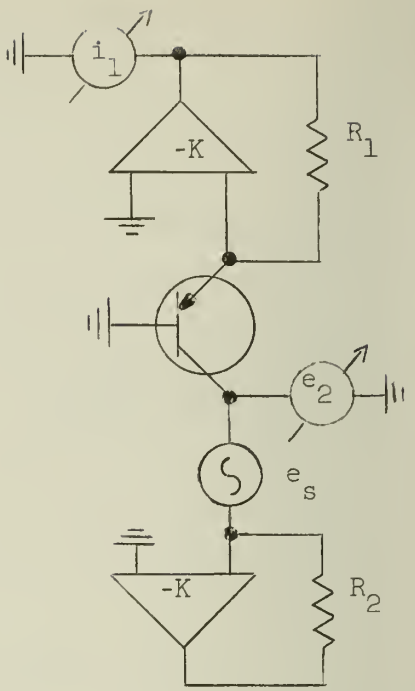

(b) Measurement of y_{12}

$$y_{12} = \frac{i_1}{e_2}$$

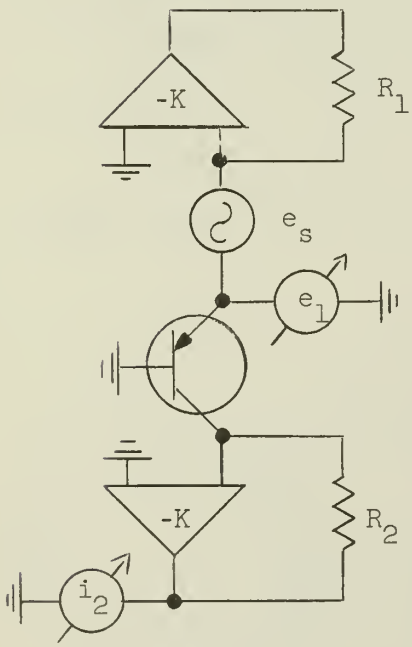

(c) Measurement of y_{21}

$$y_{21} = \frac{i_2}{e_1}$$

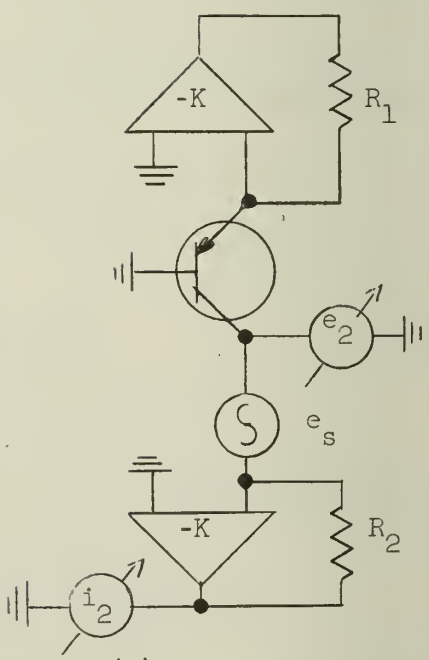

(d) Measurement of y_{22}

$$y_{22} = \frac{i_2}{e_2}$$

Figure 4. Y-Parameter Measurement

All meters are VTVM's

Here,

$$e_0 = + \frac{K}{K + 1} Ri_{in},$$

So that, if K is large,

$$e_0 \approx Ri_{in} \tag{5}$$

Consequently, the four admittance parameters can be measured with the arrangements shown in Fig. 4.

3. Direct Measurements of r_B and $(r_C + r_B)$

As explained in Section 4, it was necessary to measure r_B and $(r_C + r_B)$ directly. This was easily done as follows:

The emitter of the transistor was biased from the collector of another transistor, so that the AC load impedance (at the emitter side) seen from the collector would be very large.

An AC current (small signal) i_C was fed into the collector, and then the collector and emitter voltages were measured. See Fig. 5.

4. Comments

Obviously, the feedback resistors R_1 and R_2, respectively, in the measurements of y_{22} and y_{11} are superfluous, but even with them present the input impedances of the amplifiers are so low that it is not necessary to eliminate them, and the instrument is simpler if we let the feedback resistors connected once and for all to the amplifiers. Using these ideas, we constructed an instrument in which a bias emitter current up to $\pm$ 100 ma, and a collector voltage up to $\pm$ 5 volts could be applied to a transistor.

The amplifiers were two Philbrick K2-W operational amplifiers, which are difference amplifiers with a nominal gain of 15,000 (open loop), and the feed-back resistors were of 1kΩ. Input capacitors of 100 μf had to be used with the amplifiers to avoid the practical difficulties of keeping the amplifiers ballanced. Since, at the desired output voltage levels, the

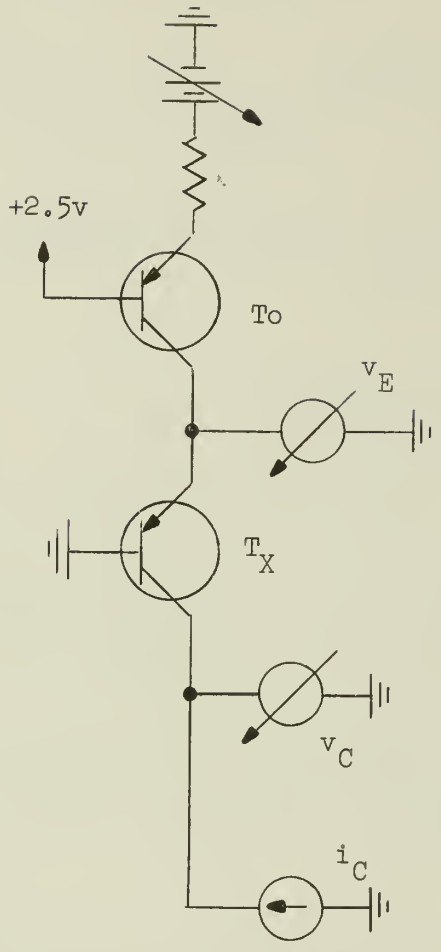

Figure 5. Measurement of r_B and $(r_C + r_B)$:

$$r_B = \frac{v_E}{i_C} \qquad ; \qquad (r_B + r_C) = \frac{v_C}{i_C}$$

Observe: Collector biasing circuit not shown

K2-W cannot handle the currents required by a 1kΩ feedback resistor, each amplifier fed a transistor emitter-follower from which the feedback was taken.

Switches provided for the measurement of all voltages (output voltages corresponding to currents in ma) with the same voltmeter, and for the insertion of the voltage source e_S (transformer secondary) at the desired point (emitter or collector).

The emitter biasing arrangement was as shown in Fig. 5, so that, by merely disconnecting the difference amplifier at the emitter side of the test transistor, r_B and $(r_C + r_B)$ could be measured as explained in Section 3.

5. Experimental Results

(a) General Remarks

Measurements were made at a frequency of 500 cps.

Short circuit voltage vs. current measurements furnish Table 1, where the region of saturation is determined.

In the region labeled "Not Saturated", the parasitic capacitive current, even at the low frequency used, is of the order of magnitude of the transistor currents, so the results are meaningless. This is so because the impedance level of r_C is large, and the parasitic capacitances of the instrument were also relatively large.

This is irrelevant since we are concerned only with the saturation region, where the impedance levels of the transistor are much lower than the impedance levels of parasitic capacitances. So, in the remaining tables, we consider only the saturation region.

The region labeled "super-saturation" is divided into two regions labeled $|G_I| < 1$ and $|G_I| > 1$; in the latter, another phenomenon occurs: The alternate current fed into the collector is amplified, and a larger current is measured from the emitter. This effect overshadows the measurements of parameters, so we eliminate this region from our study of saturation. This supersaturation phenomenon of backward current amplification (inverse current gain) will be discussed separately in PART II.

(b) Tables of Data

Table 2 is constructed from the data on Table 1. In this table Δ^y is included for checking purposes only, because the values of Δ^y obtained directly from the y's is too inaccurate, since it involves the subtraction of two quantities of the same order of magnitude: $\Delta^y = y_{11}y_{22} - y_{12}y_{21}$

The values of Δ^y are better determined by the formulas:

$$\Delta^y = \frac{y_{11}}{r_C + r_B} \qquad \text{or} \qquad \Delta^y = -\frac{y_{12}}{r_B} \qquad (6)$$

which do not involve differences, but demand direct measurements of $(r_C + r_B)$ or of r_B. The two formulas (Eqs. 6) are theoretically equivalent, but in practice the error involved in the first one is somewhat smaller as shown by the following approximate analysis:

The emitter terminals are not really open; in fact, the output impedance of transistor T_O (see Fig. 5) is even relatively low (with respect to its normal values) due to the large currents (and consequently small voltages forced by maximum dissipation) under which it operates. Then a small current i_E will be present at the emitter of T_X, which will cause an error in the measurements of both r_B and $(r_B + r_C)$, since we are neglecting its existence.

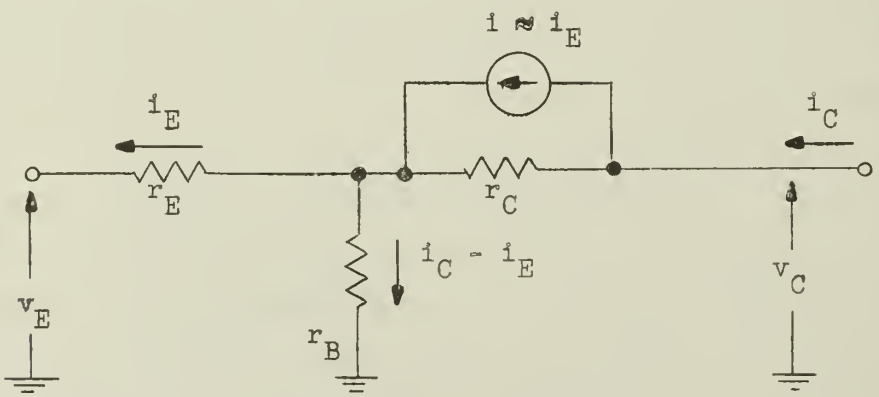

Figure 6. Approximate Equivalent Circuit

From Fig. 6, we have:

$$v_C = (i_C - i_E)(r_C + r_B) \qquad \text{and} \qquad v_E = r_B (i_C - i_E) - r_E i_E$$

So that:

$$(r_C + r_B) = \frac{v_C}{i_C - i_E} \qquad \text{and} \qquad r_B = \frac{v_E + r_E i_E}{i_C - i_E}$$

Or, by way of approximation

$$(r_C + r_B) \approx \frac{v_C}{i_C} \left(1 + \frac{i_E}{i_C}\right) \qquad \text{and} \qquad r_B \approx \frac{v_E}{i_C} \left[1 + \frac{i_E}{i_C} \left(1 + r_E \frac{i_C}{v_E}\right)\right]$$

The values we will use are: $(r_C + r_B)' = \frac{v_C}{i_C}$ and $r_B' = \frac{v_E}{i_C}$

So that, since $r_B' \approx r_B$:

$$(r_C + r_B) \approx (r_C + r_B)' \left(1 + \frac{i_E}{i_C}\right) \quad \text{and} \quad r_B \approx r_B' \left[1 + \frac{i_E}{i_C} \left(1 + \frac{r_E}{r_B}\right)\right]$$

And the relative errors will be, approximately

$$\epsilon_{CB} \approx \frac{(r_C + r_B) - (r_C + r_B)'}{(r_C + r_B)'} \approx \frac{i_E}{i_C} \quad \text{and} \quad \epsilon_B \approx \frac{r_B - r_B'}{r_B'} \approx \frac{i_E}{i_C} \left(1 + \frac{r_E}{r_B}\right) \qquad (7)$$

Consequently,

$$\epsilon_B \approx \epsilon_{CB} \left(1 + \frac{r_E}{r_B}\right), \text{ i.e., } \epsilon_{CB} < \epsilon_B \qquad (8)$$

We therefore select the first formula. It is easy to see from the tables that:

(a) The values furnished by this formula are closer to the values obtained for Δ^y from the y parameters.

(b) The second formula tends to produce smaller values for Δ^y (about 10% smaller).

Table 3 presents the measurements of current vs. voltage in the open emitter configuration as explained in No. 3. Table 4 is obtained from Table 3. Table 5 is just an intermediate step to Table 6, which is our final result.

The formulas used in the calculation of the tables are shown below for completeness:

Table 1 - $v_2 = 0$; i_1, v_2, v_1 directly measured

$v_1 = 0$; i_1, i_2, v_2 directly measured

Table 2 (from Table 1) -

$$y_{11} = \left.\frac{i_1}{v_1}\right|_{v_2=0} \quad ; \quad -y_{12} = \left.\frac{i_1}{v_2}\right|_{v_1=0}$$

$$\Delta^y = y_{11}\, y_{22} - y_{12}\, y_{21}$$

$$-y_{21} = \left.\frac{i_2}{v_1}\right|_{v_2=0} \quad ; \quad y_{22} = \left.\frac{i_2}{v_2}\right|_{v_1=0}$$

Table 3 - $i_1 = 0$; i_2, v_2, i_1 directly measured

Table 4 (from Table 3) -

$$r_B = \left.\frac{v_1}{i_2}\right|_{i_1=0} \quad , \quad r_C + r_B = \left.\frac{v_2}{i_2}\right|_{i_1=0}$$

Table 5 -

$y_{22} + y_{12}$ from Table 2; $\Delta^y = \dfrac{y_v}{r_C + r_B}$

$y_{12} - y_{21}$ from Tables 2 and 4

$y_{11} + y_{12}$

Table 6 -

$r_E = \dfrac{y_{22} + y_{12}}{\Delta^y}$ and $= \dfrac{y_{12} - y_{21}}{y_{11} + y_{12}}$, from Table 5

r_B and r_C from Table 4.

ENTRIES (volts and ma) - absolute values $v_2 = 0$: input i_1; $v_1 = 0$: input v_2

with $v_2 = 0$, $v_1 = 0$	input i_1=.5 i_2 v_1 / i_1 i_2 v_2=.10 .01	$-V_C$ (volts) 0.50			0.75			1.00			
	I_E 5	.5	.495	.00395		.495	.00395		.495	.00390	NOT SATURATED
	(ma)	.0111	.0114	.10	.104	.0108		.0102	.0105		
	10		.495	.00258		.495	.00256		.495	.00254	
		.0254	.0260		.0230	.0233		.0222	.0227		
	15		.492	.00230		.495	.00205		.495	.00203	
		.228	.233		.0420	.0427		.0372	.0380		
	20		.485	.00340		.495	.00207		.495	.00180	
		.895	.910		.260	.268		.0660	.0685		
	25		.470	.00470		.485	.00320		.495	.00215	SATURATION
		1.29	1.32		.790	.805		.295	.300		
	30		.450	.00500		.475	.00430		.485	.00303	
	Note change in v_2	.148	.157	.01	.123	.127		.079	.081		
	35		.430	.00470		.455	.00500		.475	.00420	
		.118	.137		.140	.147		.114	.118		
	40		.403	.00315		.440	.00523		.458	.00502	
		Too Unstable-Supersat.			.138	.150		.132	.138		
	45		.365	.00142		.415	.00495		.440	.00540	
		.30	.15	.01	.115	.135		.135	.145		
	50		.335	.00137		.405	.00375		.430	.00545	
		.282	.108		.013	.06		.130	.143		
	55		.315	.00135		.365	.00130		.415	.00525	
	$\lvert I_E \rvert \leq 1$	.248	.0770		.440	.266		.105	.126		
	60		.295	.00148		.325	.00093		.390	.00360	
		.190	.0685		.465	.245		.013	.043		
	65		.277	.00152		.305	.00123		.330	.00033	SUPER-SATURATION
		.164	.083		.325	.130		.820	.493		
	70		.265	.00154		.285	.00125		.305	.00065	
		.148	.098		.280	.860		.530	.270		
	75		.255	.00152		.270	.00134		.290	.00100	
		.134	.112		.235	.071		.360	.146		
	80		.245	.00154		.262	.00138		.278	.00117	
		.122	.132		.204	.074		.302	.105		
	85		.235	.00152		.250	.00142		.265	.00123	
		.117	.134		.184	.081		.264	.075		
	90		.230	.00154		.240	.00146		.255	.00130	
	$\lvert I_E \rvert \geq 1$	.110	.147		.170	.092		.237	.070		
	95		.220	.00153		.230	.00148		.245	.00136	
		.103	.153		.160	.100		.218	.071		
	100		.215	.00154		.227	.00148		.235	.00143	
		.100	.162		.145	.110		.195	.078		

Table 1. Short Circuit Measurements

ENTRIES: y's in mv; Δ^y in $(mv)^2$

y_{11} $-y_{12}$ $-y_{21}$ y_{22} Δ^y	$-V_C$ (volts) 0.50			0.75			1.00		
I_E (ma) 20	147.1	8.95							
	142.7	9.10	62.0						
25	106.3	12.9		156.2	7.90		232.5	2.95	
	100.0	13.2	115.0	151.5	8.05	61.0	230.0	3.00	20.0
30	100.0	14.8		116.2	12.3		165.0	7.90	
	90.0	15.7	268.0	110.5	12.7	115.0	160.0	8.10	89.0
35	116.3	11.8		100.0	14.0		119.0	11.4	
	91.5	13.7	516.0	91.0	14.7	197.0	113.0	11.8	117.0
40				95.6	13.8		99.7	13.2	
				84.2	15.0	272.0	91.3	13.8	171.0
45				101.0	11.5		92.6	13.5	
				83.8	13.5	400.0	81.5	14.5	242.0
50							91.7	13.0	
							78.9	14.3	299.0
55							95.2	10.5	
							79.1	12.6	368.0
60							138.8	1.3	
							108.3	4.3	456.0

Table 2. y-parameters from Table 1

$$y_{11} = \frac{i_1}{v_1}\Big|_{v_2=0} \qquad -y_{12} = \frac{i_1}{v_2}\Big|_{v_1=0}$$

$$-y_{21} = \frac{i_2}{v_1}\Big|_{v_2=0} \qquad y_{22} = \frac{i_2}{v_2}\Big|_{v_1=0} \qquad \Delta^y = y_{11}y_{22} - y_{12}y_{21}$$

ENTRIES: i_2 in ma; v_2 in volts (absolute values)

i_2	v_1	$-V_C$ (volts) 0.50		0.75		1.00	
I_E (ma) 20		.0425	.0074				
25		.1175	.01325	.380	.0064	.0100	.0019
30		.232	.0155	.102	.0138	.0395	.0063
35		.332	.0117	.182	.0152	.094	.0107
40				.272	.0158	.170	.0147
45				.340	.0124	.240	.0160
50						.298	.0149
55						.390	.100
60						.600	.087

Table 3. Open Emitter Measurements

i_2 and v_1 with $i_1 = 0$ and $v_2 = 0.1$ volts

. Entries: Ω

r_B	$(r_C + r_B)$	$-V_C$ (volts) 0.50		0.75		1.00	
I_E	20	174.0	2350			(*) Inaccurate * Unstable	
(ma.)	25	112.8	851	168.4	2630	190.0 (*)	10000
	30	66.8	431	135.2	980	159.5	2530
	35	35.3	301	83.5	549	113.8	1064
	40			56.1	368	86.5	588
	45			36.5	294	66.7	417
	50					50.0	335.5
	55					25.6*	256.5
	60					14.5*	166.5

Table 4. r_B and $(r_C + r_B)$ from Direct Measurements on Table 3. Neglect this row

$$r_B = \frac{v_1}{i_2}\bigg|_{i_1=0} \; ; \quad (r_C + r_B) = \frac{v_2}{i_2}\bigg|_{i_1=0}$$

ENTRIES: y's in mv; Δ^y in $(mv)^2$

$y_{11}+y_{12}$ / $y_{22}+y_{12}$	$y_{12}-y_{21}$ / Δ^y	$-V_C$ (volts) 0.50		0.75		1.00	
I_E (ma)	20	138.1	133.7				
		0.15	62.5				
	25	93.4	87.1	148.3	143.6	229.5	227.0
		0.30	125	0.15	59.4	0.05	23.5
	30	85.2	75.2	103.9	98.2	157.1	152.1
		0.90	232	0.40	119	0.20	65.2
	35	104.5	89.7	86.0	77.0	107.6	101.6
		1.9	385	0.70	182	0.40	112
	40			81.8	70.4	86.5	78.1
				1.2	260	0.60	170
	45			89.5	72.3	79.1	68.1
				2.0	344	1.0	222
	50					78.7	65.9
						1.3	272
	55					84.7	68.6
						2.1	371

Table 5. Intermediate Step for Table 6; y's from Table 2; $\Delta^y = \dfrac{y_{11}}{r_C + r_B}$ with $(r_C + r_B)$ from Table 4

ENTRIES: r's in Ω; I_C in ma

r_E r_C	r_B α	I_C	$-V_C$ (volts) 0.50			0.75			1.00		
I_E (ma)	20		2.4	174							
			2176	.967	19.2			19.2			19.2
	25		2.4	113		2.5	168		2.1	190	
			738	.933	24.3	2462	.968	24.5	9810	.989	24.5
	30		3.9	66.8		3.4	135		3.1	160	
			364	.883	29.2	845	.946	29.4	2370	.968	29.6
	35		4.9	35.3		3.8	83.5		3.6	114	
			266	.858	33.5	465	.895	34.0	950	.945	34.4
	40					4.6	56.1		3.5	86.5	
					37.4	312	.861	38.2	501	.903	38.7
	45					5.8	36.5		4.5	66.7	
					41.0	257	.807	42.6	350	.862	43.3
	50								4.8	50.0	
					44.9			46.7	286	.838	47.4
	55								5.7	25.6	
					47.6			50.3	231	.810	51.7

Table 6. Final Results: $r_E = \frac{y_{22} + y_{12}}{\Delta^y}$ and $\alpha = \frac{y_{12} - y_{21}}{y_{11} + y_{12}}$, From Table 5

I_C directly measured and r_B and r_C from Table 4.

Obs.: Notice that, since $y_{22} \approx -y_{12}$, $y_{22} + y_{12}$ is a small number, and the accuracy obtained for r_E is very poor. Of course r_E should be measured in a more direct manner if accurate values are desired. But here we are only concerned with a first approximation to r_E, because it is a relatively unimportant parameter with respect to saturation. The important parameters (in this order) are r_C, α and r_B, which have been measured as accurately as possible.

So, assume an error of ± 20% in the values of r_E. All the other parameters are presented with an experimental error of approximately ± 5%.

(c) Graphs

Graphs 1 to 4 present respectively r_E, r_B, α and r_C vs I_E, with V_C as a parameter.

Graph 5 is made for the purpose of comparison. The curves on the left hand side are r_C vs. I_E and α vs. I_E, and it is clear that the variation (degeneration) of r_C exceeds by far that of α. The curves at the right hand side represent r_C vs. I_C.

(d) Empirical Formula for r_C

We can see that an empirical formula can be used to calculate r_C approximately from 3 points:

$$r_C = A(I_E)^{-b} + r_C^o \qquad \ldots \qquad (9)$$

One measurement at very high values of I_E would furnish r_C^o; two measurements at moderately high values of I_E would furnish A and b; a third measurement at moderately high values of I_E could be made, if necessary, to insure that the values obtained are correct (as a check to the formula, and to insure all measurements have been made in the saturation region). Since only approximate values are desired, I_C could be used instead of I_E, with essentially the same results.

A and b are seen to be functions of V_C. So, if we wish to find r_C as a function of both V_C and I_E, we need A and b vs. V_C. However, a somewhat easier form to use would be

$$r_C \left(\frac{I_E}{I_A}\right)^{-b} (\Omega) + r_C^o \qquad \ldots \qquad (10)$$

Graphs 6 show how I_A and b vary with V_C (6a and 6b respectively). In our case, for example, we find from Graphs 6:

$$\text{From 6b:} \quad b \approx 4 \times 2^{|V_C|} = 4 \times e^{\frac{|V_C|}{0.693}}$$

$$\text{From 6a:} \quad I_A \approx 1.27 \times \lg_e \frac{|V_C|}{0.23} \qquad (11)$$

NO. 340 ·20 DIETZGEN GRAPH PAPER
20 X 20 PER INCH

EUGENE DIETZGEN CO.
MADE IN U. S. A.

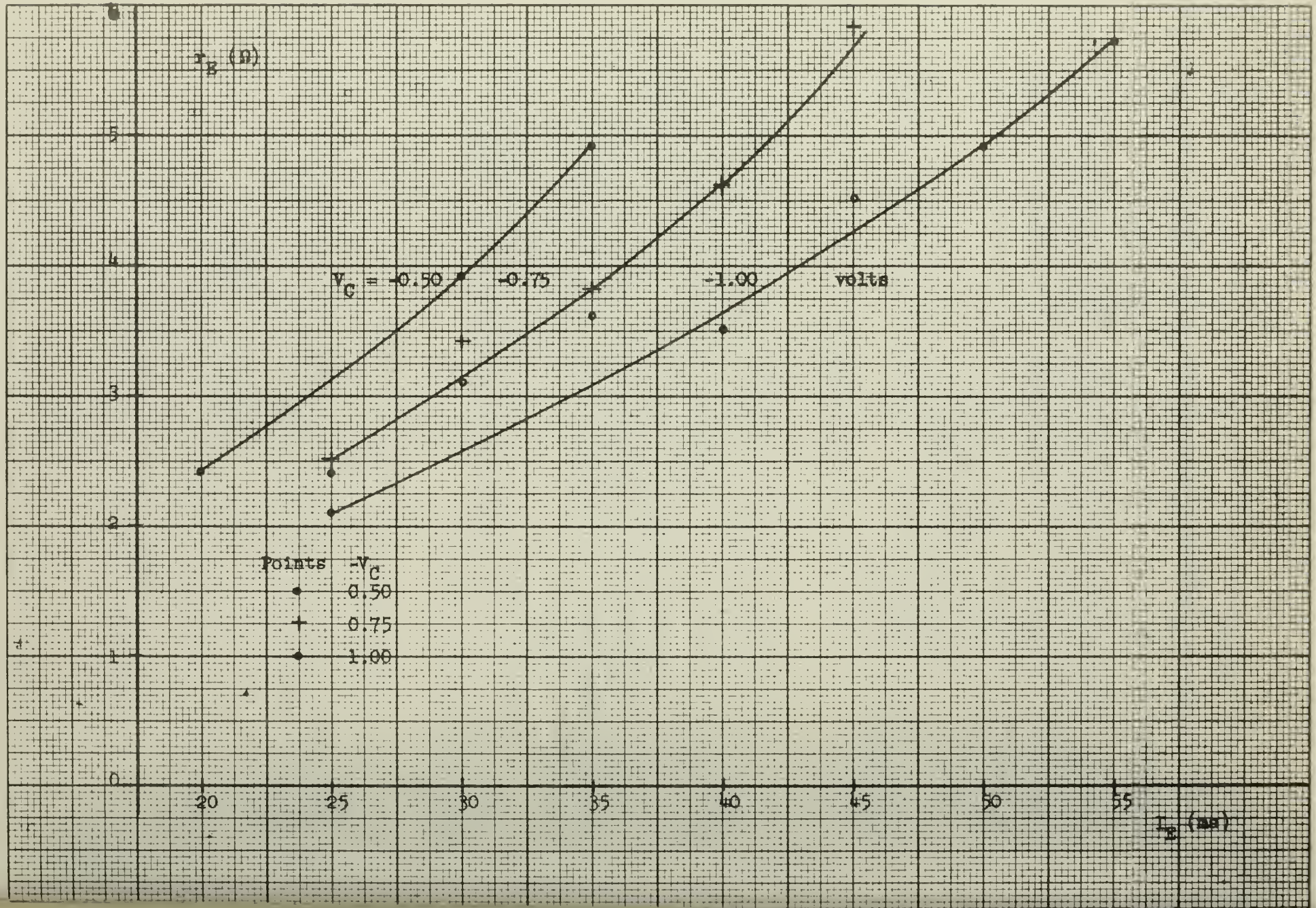

Graph 1

NO. 340 -20 DIETZGEN GRAPH PAPER
20 X 20 PER INCH
EUGENE DIETZGEN CO.
MADE IN U. S. A.

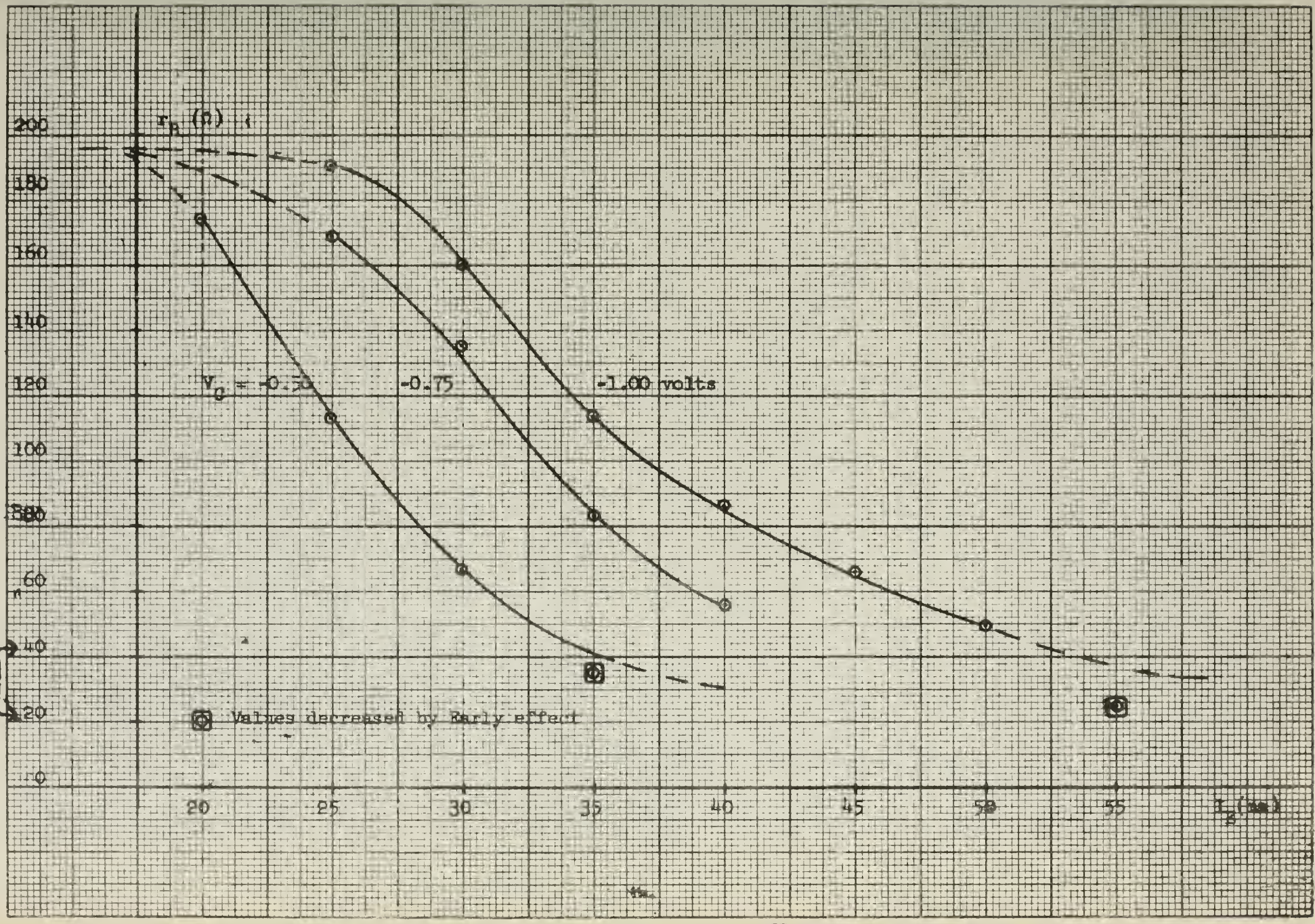

Graph #1

NO. 340 ·20 DIETZGEN GRAPH PAPER
20 X 20 PER INCH

EUGENE DIETZGEN CO.
MADE IN U. S. A.

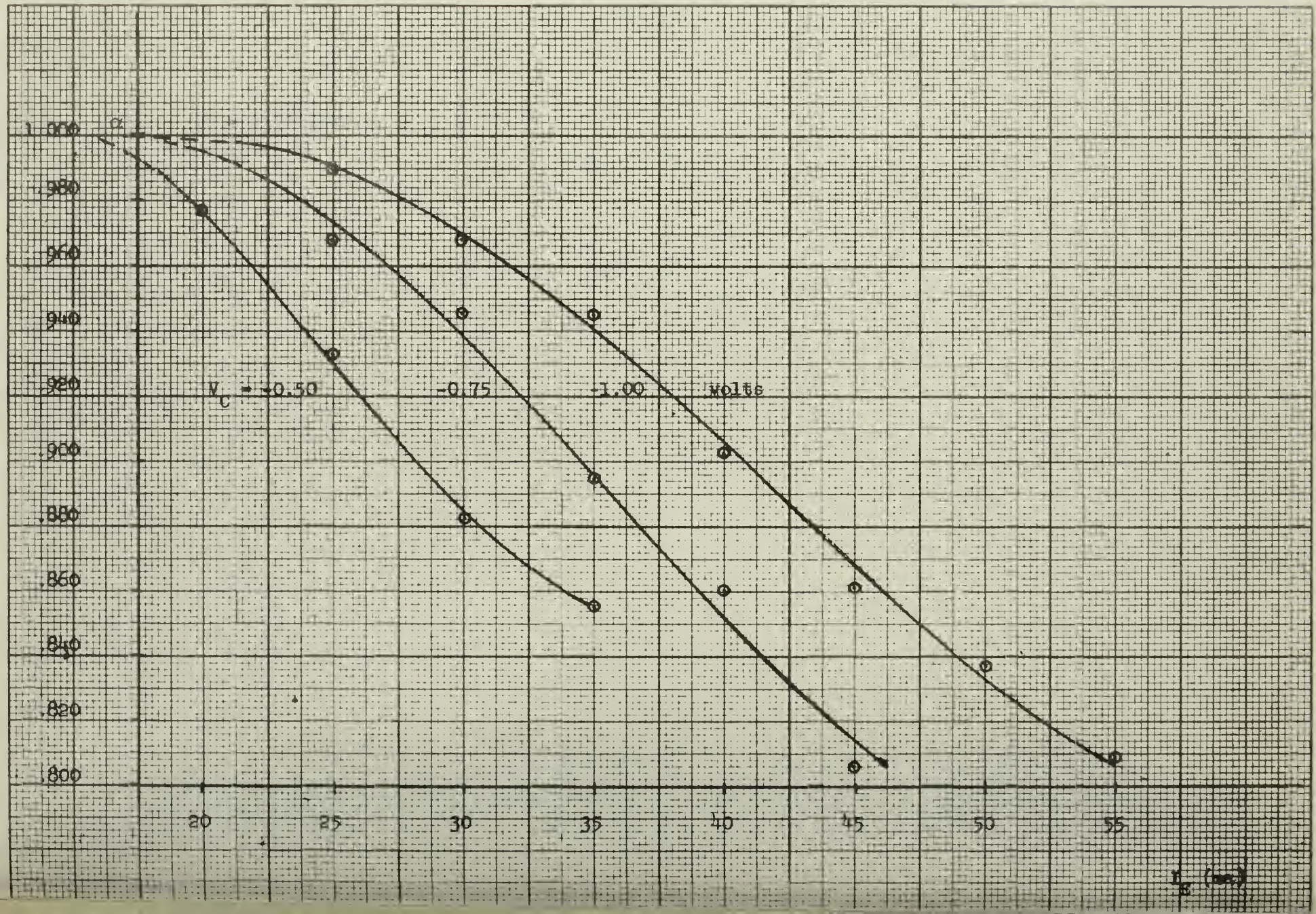

Graph 3

NO. 340 20 DIETZGEN GRAPH PAPER
20 X 20 PER INCH
EUGENE DIETZGEN CO.
MADE IN U. S. A.

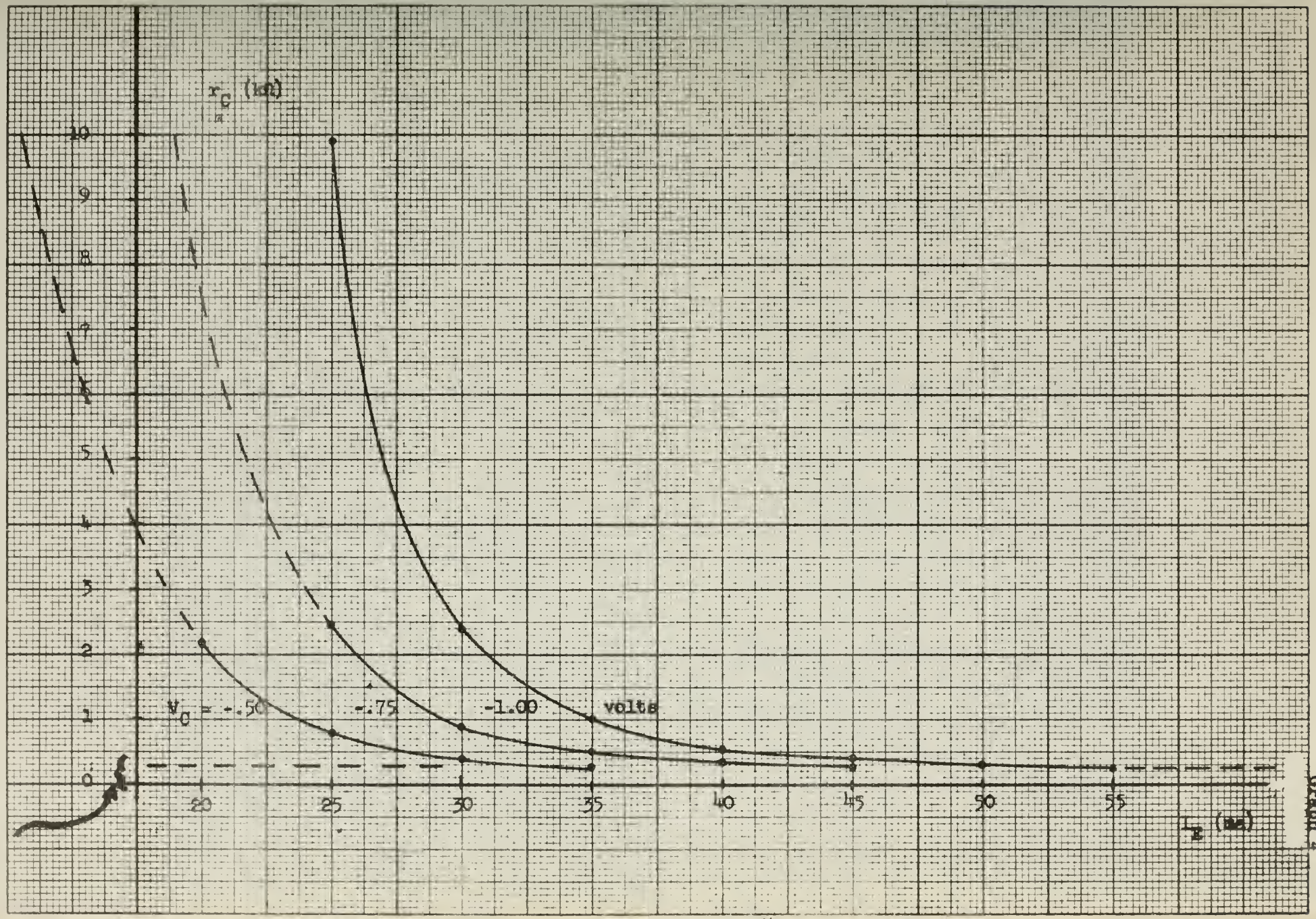

Graph 4

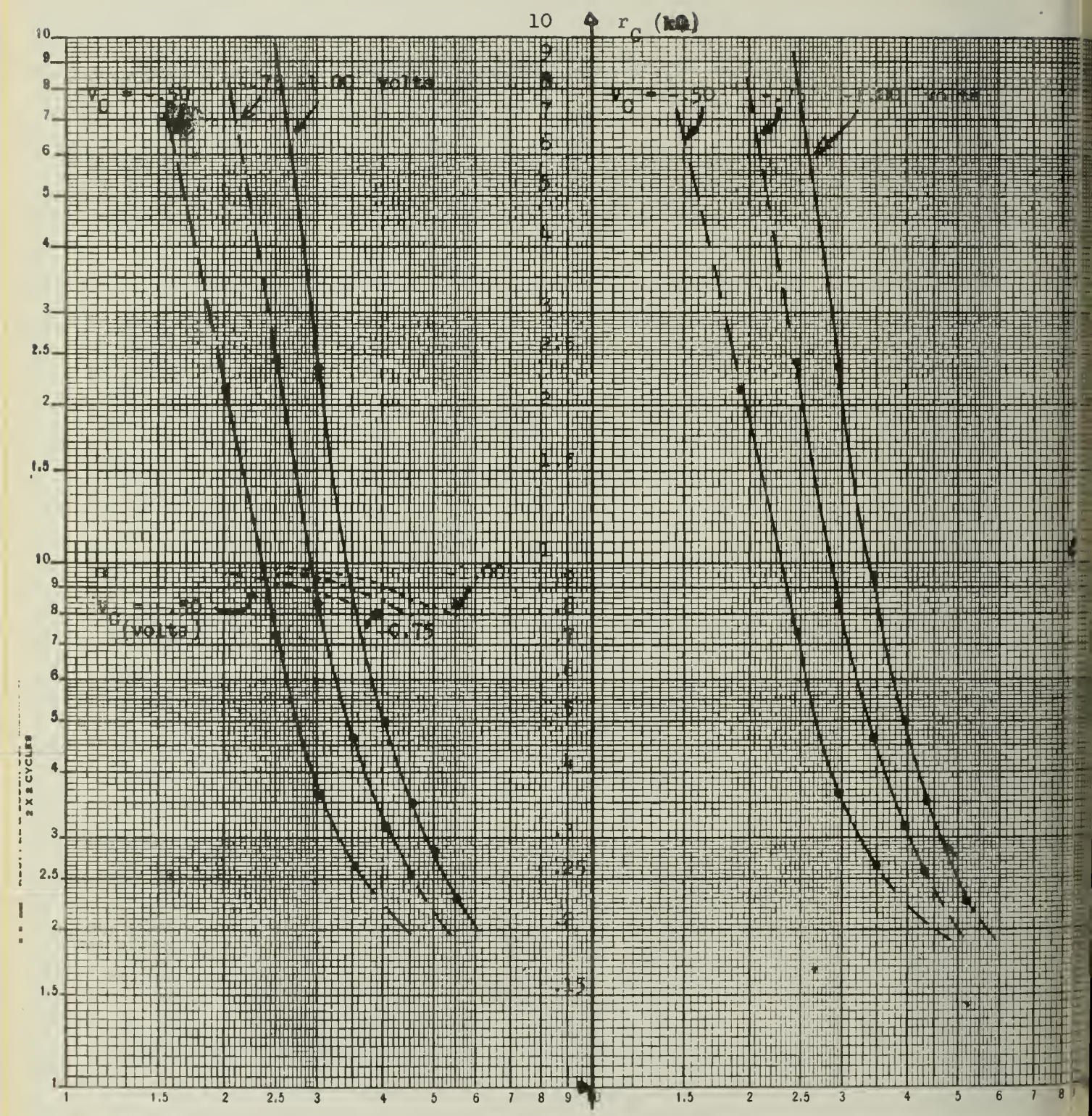

I_E (units of 10 ma)

——— Measured

— — Extrapolation (Expected)

----- α

I_C (units of 10 ma)

Graph 6.

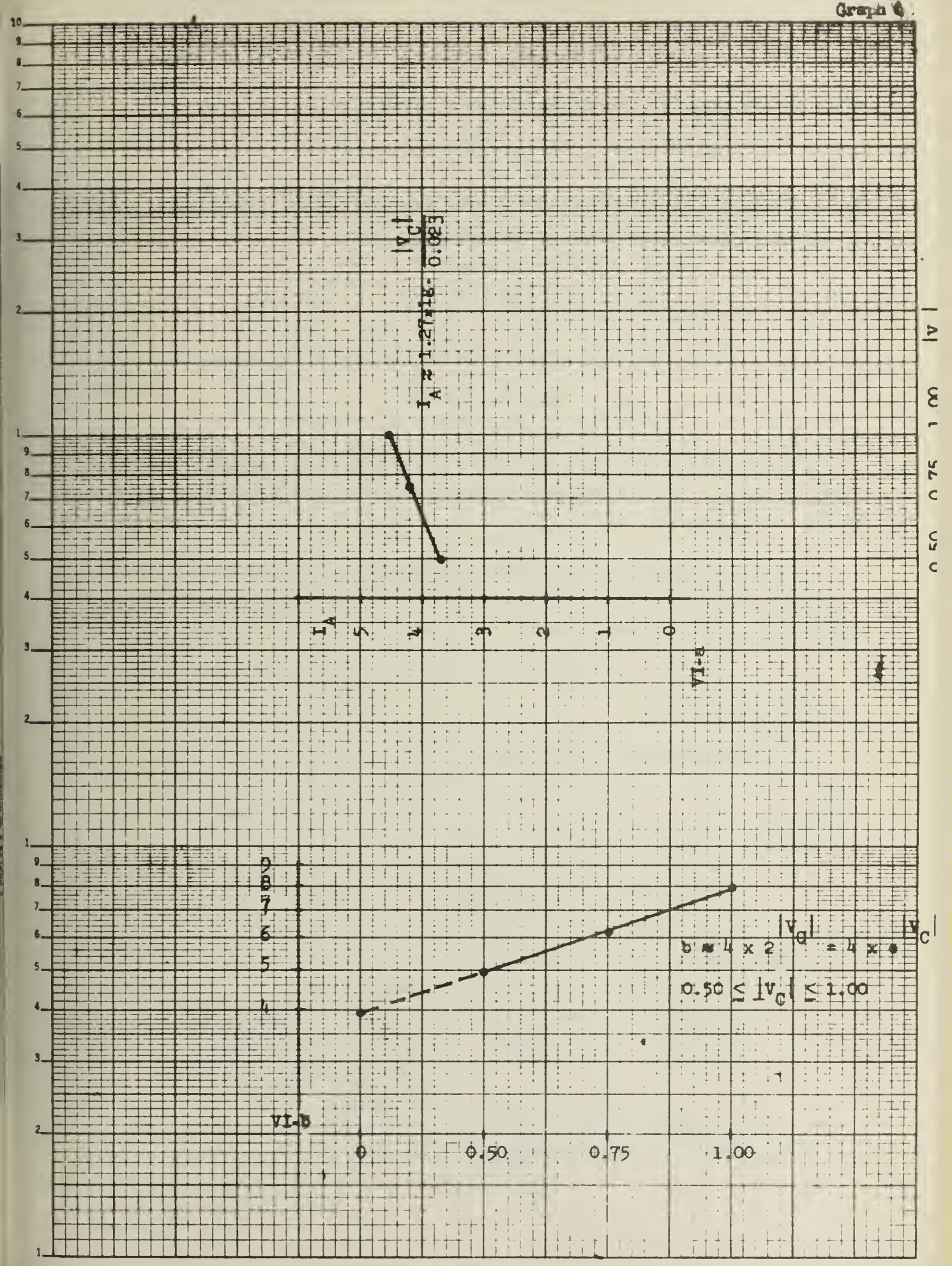
$|V_C|$
$I_A = 1.27 \times 18.0 \times 0.023$
I_A
5
4
3
2
1
0
VI-A
$|V_C|$
$|V_C|$
$b = 4 \times 2 = 4 \times a$
$0.50 \leq |V_C| \leq 1.00$
VI-B
0
0.50
0.75
1.00

which are the empirical formulas valid in the interval

$$0.50 \leq |V_C| \leq 1.00$$

So, we suspect that under saturation the parameter r_C would in general obey an empirical formula as in Eq. 1 above, with

$$b = B \cdot e^{\frac{|V_C|}{V_B}}$$

$$I_A = D \cdot \lg_e \frac{|V_C|}{V_D} \qquad (12)$$

If this is so, four measurements would give us the four constants B, V_B, D and V_D, and a fifth measurement would furnish r_C^o, the bulk resistance of the collector.

However, since the formula is empirical, only mathematical analysis or statistical data would prove or disprove it. No doubt it holds to a good approximation for our sample case.

6. Theoretical Analysis

The following analysis, made for an idealized one-dimensional transistor, does not take geometry into account, and so we cannot expect quantitative results. However, it should provide good qualitative explanation of the experimental results.

(a) Time-Independent Solution

The time-independent diffusion equation for holes in n-region is, in the one-dimensional case:

$$L_p^2 \frac{d^2 p_n(x)}{dx^2} - p_n^- (x) = -p_n^o \quad \ldots \text{ where } p_n^o \text{ is the thermal equilibrium hole density in the n-region} \qquad (13)$$

The boundary conditions in the case of the n-type base of a p-n-p transistor are

$$p_n^-(a) = p_n^o e^{\eta v_C} \quad \ldots \quad \text{where "a" is the base width} \tag{14a}$$

v_e and v_C are respectively the voltages across emitter and collector junctions, and the constant η is $\eta = \frac{q}{kT}$

$$p_n^-(0) = p_n^o e^{\eta v_E} \tag{14b}$$

The solution to the differential equation 13 is:

$$p_n^-(x) = A \sinh \frac{x}{L_p} + B \cosh \frac{x}{L_p} + p_n^o \tag{15}$$

Considering the boundary conditions we have:

From 14b: $p_n(0) = B + p_n^o = p_n^o e^{\eta v_E} = D \qquad B = p_n^o (e^{\eta v_E} - 1)$

From 14a: $p_n(a) = A \sinh \frac{a}{L_p} + B \cosh \frac{a}{L_p} + p_n^o = p_n^o e^{\eta v_C}$

$$= A \sinh \frac{a}{L_p} + p_n^o \left\{ (e^{\eta v_E} - 1) \cosh \frac{a}{L_p} + 1 \right\}$$

So $$A = \frac{p_n^o \left\{ e^{\eta v_C} - (e^{\eta v_E} - 1) \cosh \frac{a}{L_p} + 1 \right\}}{\sinh \frac{a}{L_p}}$$

Hence: $$p_n^-(x) = \frac{p_n^o \sinh \frac{a}{L_p} + p_n^o (e^{\eta v_C} - 1) \sinh \frac{x}{L_p}}{\sinh \frac{a}{L_p}} +$$

$$+ \frac{p_n (e^{\eta v_E} - 1) \left(\cosh \frac{x}{L_p} \sinh \frac{a}{L_p} - \cosh \frac{a}{L_p} \sinh \frac{x}{L_p} \right)}{\sinh \frac{a}{L_p}}$$

Or, finally:

$$\bar{p_n}(x) = p_n^o + \frac{p_n^o(e^{\eta v_C} - 1)\sinh\frac{x}{L_p} + p_n^o(e^{\eta v_E} - 1)\sinh\frac{a - x}{L_p}}{\sinh\frac{a}{L_p}} \quad (16)$$

(b) Time Dependent Diffusion Equation

The diffusion equation is:

$$L_p^2 \frac{\partial^2 p_n(x,t)}{\partial x^2} - \tau_p \frac{\partial p_n(x,t)}{\partial t} - p_n(x,t) = -p_n^o \quad (17)$$

Suppose that the boundary conditions are of the form:

$$v_E = \bar{v_E} + \tilde{v_E} \quad ; \quad v_C = \bar{v_C} + \tilde{v_C} \quad ,$$

where the symbols $\bar{}$ and $\tilde{}$ indicate respectively DC and alternate components.

So that, if $v_E << \bar{v_E}$ and $\tilde{v_C} << \bar{v_C}$; with $p(x,t) = \bar{p}(x) + \tilde{p}(x,t)$:

$$p_n(0,t) = p_n^o e^{\eta \bar{v_E}} \cdot e^{\eta \tilde{v_E}} \approx p_n^o e^{\eta \bar{v_E}} + \eta p_n^o e^{\eta \bar{v_E}} \cdot \tilde{v_E}$$

$$p_n(a,t) = p_n^o e^{\eta \bar{v_C}} \cdot e^{\eta \tilde{v_C}} \approx p_n^o e^{\eta \bar{v_C}} + \eta p_n^o e^{\eta \bar{v_C}} \cdot \tilde{v_C}$$

i.e.

$$p_n(0,t) = p_n^o e^{\eta \bar{v_E}}(1 + \eta \tilde{v_E}) = D \quad \tilde{p_n}(0,t) = \eta p_n^o e^{\eta \bar{v_E}} \cdot \tilde{v_E} \quad \ldots \quad (18)$$

$$p_n(a,t) = p_n^o e^{\eta \bar{v_C}}(1 + \eta \tilde{v_C}) = D \quad \tilde{p_n}(a,t) = \eta p_n^o e^{\eta \bar{v_C}} \cdot \tilde{v_C} \quad \ldots \quad (19)$$

If we subtract the time-independent differential equation from the time-dependent differential equation we get:

$$L_p^2 \frac{\partial^2 \tilde{p_n}}{\partial x^2} - \tau_p \frac{\partial \tilde{p_n}}{\partial t} - \tilde{p_n} = 0 \tag{20}$$

(c) Solution of the Time Dependent Equation

We can drop all indices, for simplicity, and solve the following equation under boundary conditions:

$$L \frac{\partial^2 p}{\partial x^2} - \tau \frac{\partial p}{\partial t} - p = 0 \tag{21a}$$

$$p(0,t) = C_1 e^{jw_1 t} \quad , \quad p(a,t) = C_2 e^{jw_2 t} \tag{21b}$$

and keep in mind that: $p = \tilde{p_n}(x,t)$, $L = L_p$ and $\tau = \tau_p$.

The equation is separable, so we get; with

$$p = X(x) \cdot T(t)$$

$$L^2 \frac{1}{X} \frac{\partial^2 X}{\partial x^2} - \tau \frac{1}{T} \frac{\partial T}{\partial t} - 1 = 0$$

$$\tau \frac{1}{T} \frac{\partial T}{\partial t} = K \quad ; \quad L^2 \frac{1}{X} \frac{\partial^2 X}{\partial x^2} - 1 = K \quad , \quad K = \text{a constant.}$$

Let $T = e^{jwt}$, then: ... (22)

$$\frac{\partial T}{\partial t} = jwe^{jwt} = D \quad \tau \frac{1}{T} \frac{\partial T}{\partial t} = jw\tau \quad \therefore \quad K = jw\tau$$

$$\text{So} \quad L^2 \frac{1}{X} \frac{\partial^2 X}{\partial x^2} = 1 + jw\tau \quad \therefore \quad X = e^{\frac{1}{L}\sqrt{1 + jw\tau}\, x}$$

Using the formula $\sqrt{a + jb} = \pm\left(\sqrt{\frac{C + a}{2}} + j\sqrt{\frac{C - a}{2}}\right)$, $C = |a + jb|$ we will get:

$$|1 + jw\tau| = +\sqrt{1 + w^2\tau^2} = \delta, \text{ and obviously } \delta > 1.$$

$$\text{So} \quad X = e^{\pm\left(\frac{\sqrt{(\delta + 1)/2}}{L} x + j \frac{\sqrt{(\delta - 1)/2}}{L} x\right)} \qquad \ldots \qquad (23)$$

And since any linear combination of XT is a solution, the general solution is:

$$p = Ae^{-\frac{x}{\lambda_1}} e^{j\left(w_1 t - \frac{x}{\beta_1}\right)} + Be^{\frac{x}{\lambda_1}} e^{j\left(w_1 t + \frac{x}{\beta_1}\right)} +$$

$$+ Ce^{-\frac{x}{\lambda_2}} e^{j\left(w_2 t - \frac{x}{\beta_2}\right)} + De^{\frac{x}{\lambda_2}} e^{j\left(w_2 t + \frac{x}{\beta_2}\right)} \qquad \ldots \qquad (24)$$

where $$\lambda_i = \frac{L}{\sqrt{\frac{\delta_i + 1}{2}}}, \quad \beta_i = \frac{L}{\sqrt{\frac{\delta_i - 1}{2}}}, \quad \delta_i = \sqrt{1 + w_i^2 \tau^2}, \quad i=1,2 \qquad (25)$$

(d) Periodic Boundary Conditions

To satisfy the boundary conditions, we can put the expression into a more convenient form by rearranging the constants:

$$p = \left[K_{11} e^{-\left(\frac{1}{\lambda_1} + j\frac{1}{\beta_1}\right)x} + K_{12} e^{+\left(\frac{1}{\lambda_1} + j\frac{1}{\beta_1}\right)x} \right] e^{jw_1 t} +$$

$$+ \left[K_{21} e^{-\left(\frac{1}{\lambda_2} + j\frac{1}{\beta_2}\right)x} + K_{22} e^{+\left(\frac{1}{\lambda_2} + j\frac{1}{\beta_2}\right)x} \right] e^{jw_2 t}$$

$$= p_1(x,t) + p_2(x,t) \qquad \ldots \quad (26)$$

And modify our boundary conditions:

$$\left\{ \begin{array}{l} p(0,t) = C_1 e^{jw_1 t} \\ \\ p(a,t) = C_2 e^{jw_2 t} \end{array} \right. \quad \text{become} \quad \left\{ \begin{array}{l} p_1(0,t) = c_1 e^{jw_1 t} \; ; \quad p_1(a,t) = 0 \\ \\ p_2(0,t) = 0 \; ; \quad p_2(a,t) = c_2 e^{jw_2 t} \end{array} \right. \qquad (27)$$

Hence:

$$K_{11} + K_{12} = C_1 \quad \text{and} \quad K_{11} e^{-\gamma_1 a} + K_{12} e^{+\gamma_1 a} = 0, \text{ with } \gamma_1 = \frac{1}{\lambda_1} + j\frac{1}{\beta_1}$$

Solving for K_{11} and K_{12} we get:

$$K_{11} = + \frac{C_1 e^{\gamma_1 a}}{2 \sinh(\gamma_1 a)} \; ; \quad K_{12} = - \frac{C_1 e^{-\gamma_1 a}}{2 \sinh(\gamma_1 a)}$$

So: $$p_1 = C_1 \frac{\sinh [\gamma_1(a - x)]}{\sinh (\gamma_1 a)} e^{jwt} \qquad (28)$$

Analogously:

$$K_{21} + K_{22} = 0 \text{ and } K_{21} e^{-\gamma_2 a} + K_{22} e^{+\gamma_2} = C_2, \text{ with } \gamma_2 = \frac{1}{\lambda_2} + j \frac{1}{\beta_2}$$

furnish

$$K_{21} = - \frac{C_2}{2 \sinh (\gamma_2 a)} \quad ; \quad K_{22} = + \frac{C_2}{2 \sinh (\gamma_2 a)}$$

And

$$p_2 = C_2 \frac{\sinh [\gamma_2 x]}{\sinh (\gamma_2 a)} \qquad (29)$$

And the final solution is, with p replaced by $\tilde{p_n}$:

$$\tilde{p_n}(x,t) = \frac{C_1 \sinh [\gamma_1(a - x)] e^{jw_1 t}}{\sinh (\gamma_1 a)} + \frac{C_2 \sinh [\gamma_2 x] e^{jw_2 t}}{\sinh (\gamma_2 a)} \qquad (30)$$

(e) Admittance Parameters

With

$$C_1 = \eta p_n^o e^{\eta v_E} \cdot V_E \quad \text{and} \quad C_2 = \eta p_n^o e^{\eta v_C} \cdot V_C$$

$$\tilde{v_E} = V_E e^{jw_1 t} \quad \text{and} \quad \tilde{v_C} = V_C e^{jw_2 t} \qquad (31)$$

we have:

$$\tilde{p_n}(x,t) = \frac{\eta p_n^o e^{\eta \bar{v_E}} \sinh [\gamma_1(a - x)]}{\sinh (\gamma_1 a)} \tilde{v_E} + \frac{\eta p_n^o e^{\eta \bar{v_C}} \sinh [\gamma_2 x]}{\sinh (\gamma_2 a)} \tilde{v_C} \qquad (32)$$

Since the current density $\tilde{J_p}(x,t)$ is given by:

$$\tilde{J_p}(x,t) = -qD_p \frac{\partial \tilde{p_n}}{\partial x} \qquad (33)$$

we get:

$$\tilde{J_p}(x,t) = +qD_p \eta p_n^o e^{\eta \bar{v_E}} \gamma_1 \frac{\cosh [\gamma_1(a - x)}{\sinh (\gamma_1 a)} \tilde{v_E} - qD_p \eta p_n^o e^{\eta \bar{v_C}} \gamma_2 \frac{\cosh [\gamma_2 x]}{\sinh (\gamma_2 a)} \tilde{v_C}$$

(34)

Consider that:

$$qD_p \eta p_n^o e^{\eta \bar{v_E}} = \frac{L_p}{\rho_E \times S}$$

$$qD_p \eta p_n^o e^{\eta \bar{v_C}} = \frac{L_p}{\rho_C \times S} \qquad (35)$$

where S is the area of the base and ρ_E and ρ_C are respectively the emitter and base junctions dynamic resistances if these junctions were isolated, i.e., they are the dynamic resistances calculated from the diode equation when independently applied to each junction.

Also, since $\tilde{i_p} = S\tilde{J_p}$ and if $\tilde{i} \sim \tilde{i_p}$ (neglecting electron currents from the base into emitter and collector), we get the admittance parameters from the pair of equations:

$$\tilde{i_E} = + \frac{\xi(w_1)}{\rho_E} \coth \left[\xi(w_1) \frac{a}{L_p}\right] \tilde{v_E} - \frac{\xi(w_2)}{\rho_C} \operatorname{csch} \left[\xi(w_2) \cdot \frac{a}{L_p}\right] \tilde{v_C}$$

$$\tilde{i_C} = - \frac{\xi(w_1)}{\rho_1} \operatorname{csch} \left[\xi(w_1) \frac{a}{L_p}\right] \tilde{v_E} + \frac{\xi(w_2)}{\rho_1} \coth \left[\xi(w_2) \cdot \frac{a}{L_p}\right] \tilde{v_C}$$

Because $\tilde{i_E} = \tilde{i}(0,t)$ and $\tilde{i_C} = -\tilde{i}(a,t)$

there $\xi(w_i) = L_p \gamma_i = \sqrt{\frac{\delta_i + 1}{2}} + j \sqrt{\frac{\delta_i - 1}{2}}$, $i = 1,2$.

If $w_E = w_C$, i.e., if only one signal source is applied, then $\xi = \xi(w)$ and we can write:

$$y_{11} = + \frac{1}{\rho_E} \xi \coth \left[\frac{a}{L_p} \xi\right] \quad ; \quad y_{12} = - \frac{1}{\rho_C} \xi \operatorname{csch} \left[\frac{a}{L_p} \xi\right]$$

$$y_{21} = - \frac{1}{\rho_E} \xi \operatorname{csch} \left[\frac{a}{L_p} \xi\right] \quad ; \quad y_{22} = + \frac{1}{\rho_C} \xi \coth \left[\frac{a}{L_p} \xi\right] \qquad (37)$$

$$\Delta^y = \frac{1}{\rho_E \rho_C} \xi^2 = \frac{1 + jw\tau_p}{\rho_E \rho_C} \qquad (38)$$

We should point out here that these equations are just a first approximation, since the early effect is not taken into account. In fact, the junction depletion capacitances are not considered, and the modulation of base spread resistance with variation of base width under small signals is also neglected.

These effects, however, can be very important, so we should bear in mind this restriction on the validity of the above equations.

(f) Equivalent Circuit Parameters

The equations below furnish the equivalent circuit parameters for a T-model, common base configuration. Symbols r_E^o, r_B^o and r_C^o represent bulk and contact resistances:

$$z_E = \frac{y_{22} + y_{12}}{\Delta^y} + r_E^o \quad ; \quad z_B = -\frac{y_{12}}{\Delta^y} + r_B^o$$

$$z_C = \frac{y_{11} + y_{12}}{\Delta^y} + r_C^o \quad ; \quad \alpha = \frac{y_{12} - y_{21}}{y_{11} + y_{12}} \qquad (39)$$

Substitution of the y-parameters in the above equations yields (see Fig. 7):

In general: with $w\tau p << 1$, then:

$$z_E = \frac{a\rho_E}{2L_p} + r_E^o \quad \ldots \quad (40) \qquad r_E = \frac{a\rho_E}{2L_p} + r_E^o \quad \ldots \quad (40a)$$

(Notice that z_E is always real)

$$z_B = \frac{L_p\rho_E}{a(1 + jw\tau_p)} + r_B^o \quad \ldots \quad (41) \qquad r_B = \frac{L_p\rho_E}{a} + r_B^o \quad \ldots \quad (41a)$$

$$z_C = \frac{(\rho_C - \rho_E)L_p}{a(1 + jw\tau_p)} + \rho_C \frac{a}{2L_p} + r_C^o \qquad (42)$$

$$r_C = \rho_C \frac{L_p}{a} + \frac{a}{2L_p} - \rho_E \frac{L_p}{a} + r_C^o \quad \text{or} \qquad (42a)$$

$$r_C \approx (\rho_C - \rho_E) \frac{L_p}{a} + r_C^o, \quad \text{since } a << L_p. \qquad (42b)$$

$$\alpha = \frac{1}{\left(\frac{a}{L_p}\right)^2} \qquad (43)$$
$$1 + \frac{}{2\left(1 - \frac{\rho_E}{\rho_C}\right)} (1 + jw\tau_p)$$

$$\alpha = \frac{1}{\left(\frac{a}{L_p}\right)^2} \qquad (43a)$$
$$1 + \frac{}{2\left(1 - \frac{\rho_E}{\rho_C}\right)}$$

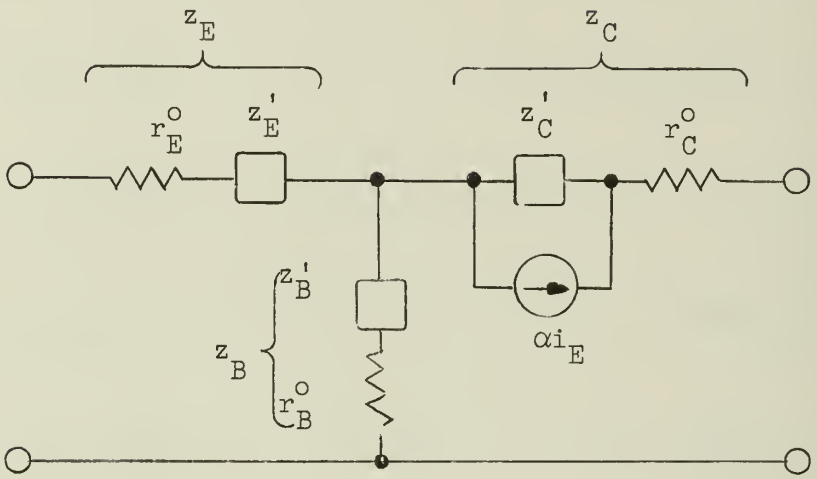

Figure 7. T-Model Approximate Equivalent Circuit for Common Base Configuration

As shown below, with the following approximations: $\sinh(x) \approx x$; $\cosh(x) \approx 1 + \frac{x^2}{2}$, if $|x| << 1$

$$z_E = \rho_E \frac{\cosh\left[\frac{a}{L_p}\xi\right] - 1}{\xi \sinh\left[\frac{a}{L_p}\xi\right]} + r_E^o \approx \rho_E \frac{1 + \left[\frac{1}{2}\left(\frac{a}{L_p}\xi\right)^2\right] - 1}{\xi\left(\frac{a}{L_p}\xi\right)} + r_E^o =$$

$$= \rho_E \frac{a}{2L_p} + r_E^o \qquad \ldots \qquad (40)$$

$$z_B = \rho_E \frac{1}{\xi \sinh\left[\frac{a}{L_p}\xi\right]} + r_B^o \approx \rho_E \frac{1}{\xi\left(\frac{a}{L_p}\xi\right)} + r_B^o =$$

$$= \rho_E \frac{L_p}{a(1 + jw\tau_p)} + r_B^o \qquad (41)$$

$$z_C = \frac{\rho_C \cosh\left[\frac{a}{L_p}\xi\right] - \rho_E}{\xi \sinh\left[\frac{a}{L_p}\xi\right]} + r_C^o \approx \frac{\rho_C - \rho_E}{\xi\left(\frac{a}{L_p}\xi\right)} + \frac{\rho_C \frac{\left(\frac{a}{L_p}\xi\right)^2}{2}}{\xi\left(\frac{a}{L_p}\xi\right)} + r_C^o =$$

$$= \frac{(\rho_C - \rho_E) L_p}{a(1 + jw\tau_p)} + \rho_C \frac{a}{2L_p} + r_C^o \quad \ldots \quad (42)$$

$$\alpha = \frac{\frac{\xi}{\rho_E}\operatorname{csch}\left[\frac{a}{L_p}\xi\right] - \frac{\xi}{\rho_C}\operatorname{csch}\left[\frac{a}{L_p}\xi\right]}{\frac{\xi}{\rho_E}\coth\left[\frac{a}{L_p}\xi\right] - \frac{\xi}{\rho_C}\operatorname{csch}\left[\frac{a}{L_p}\xi\right]} = \frac{\rho_C - \rho_E}{\rho_C \cosh\left[\frac{a}{L_p}\xi\right] - \rho_E} \approx$$

$$\approx \frac{\rho_C - \rho_E}{(\rho_C - \rho_E) + \frac{1}{2}\left(\frac{a}{L_p}\xi\right)^2 \rho_C} = \frac{1}{1 + \frac{\left(\frac{a}{L_p}\right)^2}{2\left(1 - \frac{\rho_E}{\rho_C}\right)}(1 + jw\tau_p)} \qquad (43)$$

(g) Dependence of r_C and α on ρ_E and ρ_C. $(w\tau_p << 1)$

Notice that (see Equations 35) $\rho_E = Ke^{-\eta v_E}$ and $\rho_C = Ke^{-\eta v_C}$, so really, ρ_E and ρ_C represent just a transformation of variables from

$v_E \longrightarrow \rho_E\ (v_E)$ and $v_C \longrightarrow \rho_C\ (v_C)$.

Also, $\rho_C - \rho_E = K(e^{-\eta v_C^-} - e^{-\eta v_E^-})$ ... (44) and $\frac{\rho_C}{\rho_E} = k = e^{\eta(v_E^- - v_C^-)}$ ... (45)

$$\rho_C - \rho_E = \rho_E\,(k - 1) \qquad \ldots (46)$$

Now let us write both r_C and α as functions of ρ_E and k:

$$r_C \approx \rho_E \frac{L_p}{a}\,(k - 1) + r_C^o \quad \ldots (47) \text{ and } \alpha \approx 1 - \frac{1}{2}\frac{k}{k - 1}\left(\frac{a}{L_p}\right)^2,$$

$$\text{if } \frac{1}{2}\frac{k}{k - 1}\left(\frac{a}{L_p}\right)^2 << 1 \quad \ldots (48)$$

and so we must assume $k >> 1$

Observe that:

1st) r_C depends both on ρ_E and k, but

2nd) α depends on k, and is independent of ρ_E.

Assume ρ_E is held fixed (v_E^- is fixed), and change k (v_C^- is changed).

Then, for values of $k >> 1$ (true on saturation, as long as $v^- < 0$), it is obvious that

$$r_C \approx \rho_E \frac{L_p}{a}\,(k - 1) \approx \rho_E \frac{L_p}{a}\,(e^{\eta v_E^-} \cdot e^{-\eta v_C^-} - 1) \qquad \ldots (49)$$

i.e., r_C decreases <u>exponentially</u> when $v_C^- \longrightarrow 0$, $v_C^- < 0$.

But $$\alpha = 1 - \frac{1}{2}\frac{k}{k - 1}\left(\frac{a}{L_p}\right)^2 \approx 1 - \frac{1}{2}\left(\frac{a}{L_p}\right)^2, \qquad \ldots (50)$$

i.e., α remains essentially constant as long as $k >> 1$.

In general, as k decreases ($v_C^- \longrightarrow 0$, $v_C^- < 0$), r_C decreases by orders of magnitude while α decreases of a few per cent.

However, after the value of k becomes comparable with unity, this situation changes. For this range of k we must write:

$$r_C = \rho_E \frac{L_p}{a} (k - 1) + r_C^o \quad \ldots (51) \text{ and } \alpha = \frac{1}{1 + \frac{1}{2} \frac{k}{k - 1} \left(\frac{a}{L_p}\right)^2} \quad (52)$$

We see that as $k \longrightarrow 1$, $k > 1$, $r_C \longrightarrow r_C^o$ and $\alpha \longrightarrow 0$, so we conclude that the relative change of α for small k becomes larger than the relative change of r_C. Nevertheless it is easy to see that this situation is difficult to arise in practice since $k \longrightarrow 1$ implies $v_C^- \longrightarrow v_E^-$; the measurements taken show that α is never too small in normal saturation, even in a region where r_C is essentially equal to r_C^o.

The whole discussion should be summarized by noticing that

$$\alpha = \frac{(\rho_C - \rho_E) \frac{L_p}{a}}{(\rho_C - \rho_E) \frac{L_p}{a} + \frac{1}{2} \rho_C \frac{a}{L_p} (1 + jw\tau_p)} \quad \ldots \quad (53)$$

i.e.

$$\alpha = \frac{z_C' - \rho_e \frac{a}{2L_p}}{z_C'} \quad (54)$$

Since

$$z_C' = \frac{(\rho_C - \rho_E) \frac{L_p}{a}}{(1 + jw\tau_p)} + \frac{1}{2} \rho_C \frac{a}{L_p} \quad \ldots \quad (55)$$

Then, if $w\tau_p << 1$, α is almost equal to 1 as long as $z_C' >> \rho_C \frac{a}{L_p}$, which is true if $\rho_C >> \rho_E$, an inequality that holds even at fairly

deep saturation levels, when z_C' is orders of magnitude less than its value in normal operation.

So, the parameter r_C (or rather z_C'), is the main cause for the degeneracy of transistor properties with saturation; in fact, with increasingly saturating conditions z_C' short circuits the current source αi_E while the values of α would otherwise (even at fairly deep saturation levels) still allow a useful transistor operation.

(h) Behavior of r_B and r_E

The behavior of r_B is qualitatively accounted for, since r_B is proportional to ρ_E, and consequently, a decreasing function of $\bar{v_E}$, hence a decreasing function of I_E. However, the behavior of r_E is not accounted for by this very simplified analysis. It is worth noticing that increase in the value of "a" (the base width) due to Early effect could explain the increase of r_E with deeper saturation levels.

We would like to call attention to the fact that the relation of r_E to ρ_E is very weak, in the sense that not only the values, but even the orders of magnitude are different, and clearly r_E^o plays a role as important as ρ_E in the value of r_E.

Besides, if we take Early effect into account, a different analysis must be made, so the expressions for the various parameters would be somewhat modified. This analysis is carried out in Section 7 of Part II, and the results show that, even though all other parameters are indeed modified by Early effect, r_E is not, and hence the present expression (40) remains valid. We must then conclude from experimental fact that the increase of "a" due to low collector biasing voltage and high emitter biasing currents must be large enough to offset the effect of decreasing ρ_E; besides, as is shown in the next section, L_p also decreases with saturation; since L_p appears not only as explicit denominator in

$$\frac{a\rho_E}{2L_p},$$

but also in the numerator of the expression for ρ_E itself (see Eqs. 35), it has no effect on r_E. Obviously if these considerations about "a" and "L_p" are applied to r_B its decreasing character is stressed.

As a last observation we should point out that, in order to explain the values found for r_E and r_B, we would have (in order of magnitude only):

$$\rho_E \frac{L_p}{a} \approx 10^2 \times \frac{a}{L_p} \rho_E$$

hence,

$$\frac{L_p}{a} \approx 10.$$

and, from values of r_E or r_B, for example,

$$\rho_E \approx 10\Omega.$$

(i) Variation of L_p and τ_p

It is worth noticing that L_p does not remain constant with saturation; in fact,

$$L_p = + \sqrt{D_p \tau_p} \qquad (56)$$

for a non-degenerate case (quasi-Fermi levels in the forbidden band) D_p depends only on the crystal structure, but τ_p depends also on the majority carrier concentration:

$$\tau_p = \frac{1}{p n_n} \qquad (57)$$

r is the recombination factor and $n_n = n_n^o + (\rho_n^- - \rho_n^o)$, because of charge neutrality. Hence

$$\tau_p = \frac{1}{r[(n_n^o - \rho_n^o) + p_n^-]} \tag{58}$$

But $p_n^o << n_n^o$; if $p_n << n_n^o$ also, then τ_p is constant to a good approximation, but as p_n^- increases to values comparable to n_n^o, τ_p decreases.

In general we have then:

$$L_p = +\sqrt{\frac{D_p}{r[(n_n^o - p_n^o) + p_n^-]}} \tag{59}$$

i.e., L_p decreases towards deeper levels of saturation. The large biasing base currents seem to imply that τ_p (and L_p) are orders of magnitude smaller than in normal operation.

From Table 6, for example, we see that, for $I_E = 55$ ma and $V_C = -1.00$ volts, $I_E = 51.7$ ma, i.e., $I_B = 3.3$ ma.

We have the relation:

$$I_B = qS \int_{x=0}^{x=a} \frac{\bar{\rho}_{n(x)}}{\tau_p(x)}\, dx \qquad (60)$$

i.e.

$$I_B = qSr \int_{x=0}^{x=a} [(n_n^o - p_n^o) + \bar{p}_n(x)]\, \bar{p}_n(x)\, dx \qquad (61)$$

Where q is the electron charge, S is base area and a is base width and $\bar{p}_n(x)$ is given by Equation 16.

For a convenient average value $\bar{p}_n$ of $\bar{p}_n(x)$ with respect to x, we can write:

$$I_B = qSar \left\{ (n_n^o - p_n^o)\, \bar{p}_n + \bar{p}_n^{\,2} \right\} \qquad (62)$$

Solution of (62) for $\bar{p}_n$ would furnish $\bar{\tau}_p$ and $\bar{L}_p$, which are effective values of τ_p and L_p throughout the base of the transistor, and are obtained by entering $\bar{p}_n$ instead of $\bar{p}_n$ in equations (58) and (59).

It is easy to see that, if I_B increases by orders of magnitude, then $\bar{p}_n$ must become larger than $(n_n^o - p_n^o)$; so, $\bar{\tau}_p$ and $\bar{L}_p$ must decrease accordingly.

It is interesting to notice that, for very large values of $\bar{p}_n$, say $\bar{p}_n >> n_n^o$, we would have

$$\bar{\tau}_p \sim I_B^{-1/2} \qquad \text{and} \qquad \bar{L}_p \sim I_B^{-1/4} \qquad (63)$$

Eventually, this can invalidate the often used approximation $\frac{a}{L_p} << 1$; also, these variations of L_p influence the behavior of the parameters the following way:

Notice (Equations 35) that

$$\rho_E = K \cdot L_p \cdot e^{-\eta v_E} \tag{64}$$

$$\text{and } \rho_C = K \cdot L_p \cdot e^{-\eta v_C} \tag{65}$$

$$\text{where } K = (qD_p \eta p_n^o S)^{-1} \tag{66}$$

Then, from Equations 40-43, we get:

$$z_E = \frac{a}{2} Ke^{-\eta v_E} + r_E^o \quad \ldots \quad \text{has its growth with } I_E \text{ still unexplained, but difficulties are not worse than before.} \tag{67}$$

$$z_B = \frac{KL_p^2 e^{-\eta v_E}}{a(1 + jw\tau_p)} + r_B^o \quad \ldots \quad \text{its reduction with } I_E \text{ is even sharper.} \tag{68}$$

$$z_C = \frac{K(e^{-\eta v_C} - e^{-\eta v_E}) L_p^2}{a(1 + jw\tau_p)} + Ke^{-\eta v_C} \cdot \frac{a}{2} + r_C^o \quad \ldots \quad \text{its reduction with } I_E \text{ is even sharper.} \tag{69}$$

And from Equation (54),

$$\alpha = \frac{z_C^1 - Ke^{-\eta v_C} \frac{a}{2}}{z_C^1} \quad \ldots \quad \text{its decrease with } I_E \text{ continues to be small with respect to that of } z_C. \tag{70}$$

And finally, we should point out that the base width, a, also changes with saturation levels, due to Early effect, and this should also be considered. In fact, a increases with saturation level, and this fact should explain the growth of z_E with I_E when it occurs.

The value of a is given by

$$a = a_0 - \frac{\delta_E + \delta_C}{Z}$$

where a_0 is the total width of the n-region, and δ_E and δ_C, for the case of the GF-45011 are given in Equations 12 and 13 of Part II of this report.

PART II

SUPERSATURATION

1. Introduction

It has been observed that under certain pairs of high values of emitter biasing current I_E and low values of collector biasing voltage V_C applied to mesa type transistors GF-45011 and S-166, a small amplitude alternate current fed at the collector may control a larger current in the emitter circuit. (See Table 1.)

The following has been observed about this inverse current gain:

(a) It depends on the load at the emitter. Under resistive load conditions, gains as high as 7 or 8 have been observed; gains of 60 or 70 (at the resonance frequency) have been observed in the case of a 100μf capacitive load; under short circuit conditions, if a maximum gain is attempted, the system becomes unstable.

(b) The gain (of course) depends on frequency; in the case of a resistive load it is a typical low-pass characteristic, falling at 6 db/octave after cut-off frequency; however, with a capacitive load, it presents a typical resonance characteristic. The natural frequencies are low (order of 1000 cps).

(c) The phenomenon depends very critically on the values of V_C and I_E, i.e., it occurs at a determined "saturation level", and for deeper saturation levels the output emitter currents become very small (about 1/3 of input collector current). It also depends on the sample very strongly, i.e., with a sample a maximum gain of 8 is obtained, while with the same load another sample will furnish a maximum gain of, say, 2.

It is larger with the GF-45011 than with the S-166, and occurs at less deep saturation levels with the former than with the latter.

Other types of transistors were tried, and it was found that the output emitter current would pass from the regular saturation value

(about 98% of the value of the input collector current) directly to the degenerate values of about 1/3 of the input collector current without any region of gain larger than one.

(d) The circuit used to measure the phenomenon is shown below (Fig. 1) in simplified form (biasing circuits eliminated):

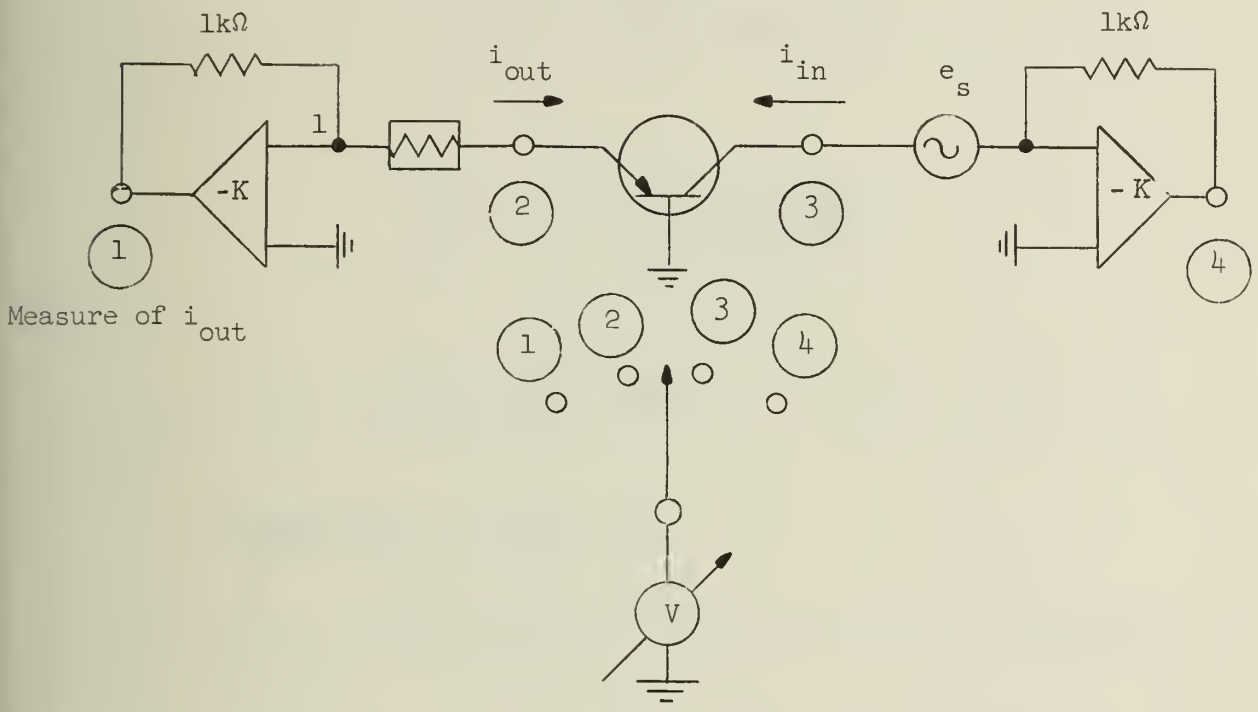

Figure 1. Measurement of Supersaturation Effects

It was noticed that instability would occur for low values of resistive load, at some regions on the I_E, V_C plane.

Also, when stable, the gain is negative (except for the usual phase shifts), with the reference directions shown in Fig. 1.

2. Attempted Explanation Neglecting the Early Effect

Then we can use the expressions found in Eqs. 37 and 38 of Part I for the y-parameters and the formula:

$$G_I = \frac{i_E}{i_C} = \frac{y_{12}}{z_E \Delta y + y_{22}}, \text{ where } z_E = z_L + r_E^o \qquad (1)$$

and get:

$$G_I = - \frac{\operatorname{csch} \left[\xi \frac{a}{L_p} \right]}{\xi \frac{z_E}{\rho_E} + \coth \left[\xi \frac{a}{L_p} \right]} \qquad (2)$$

$$= - \frac{1}{\xi \frac{z_E}{\rho_E} \sinh \left[\xi \frac{a}{L_p} \right] + \cosh \left[\xi \frac{a}{L_p} \right]}$$

If $\left| \xi \frac{a}{L_p} \right| << 1$, $\quad \sinh \left[\xi \frac{a}{L_p} \right] \approx \xi \frac{a}{L_p}$

$$\cosh \left[\xi \frac{a}{L_p} \right] \approx 1 + \frac{1}{2} \xi^2 \left(\frac{a}{L_p} \right)^2$$

Then:

$$G_I = - \frac{1}{\xi^2 \frac{z_E a}{\rho_E L_p} + 1 + \frac{1}{2} \xi^2 \left(\frac{a}{L_p} \right)^2}$$

But $\xi^2 = 1 + jw\tau_p$, so:

$$G_I = - \frac{1}{\left(1 + \frac{a z_E}{L_p \rho_E} + \frac{a^2}{L_p^2} \right) + jw\tau_p \left(\frac{a z_E}{L_p \rho_E} + \frac{a^2}{L_p^2} \right)}$$

Or, replacing jw by s:

$$G_I = \frac{1}{\left\{1 + \left(\frac{a}{L_p} + \frac{z_E}{\rho_E}\right)\frac{a}{L_p}\right\} + \left(\frac{a}{L_p} + \frac{z_E}{\rho_E}\right)\frac{a}{L_p}\tau_p s} \qquad (3)$$

It is clear that from Eq. 3 we will always have $|G_I| < 1$.

3. Interpretation through the Early Effect

If the Early effect is taken into account, the spreading resistance of the base can be expressed as:

$$r_B = \frac{R_B}{a_0 - \frac{\delta_E + \delta_C}{2}} \qquad (4)$$

where a_0 : base width if no depletion layers existed.

δ_E and δ_C : width of emitter and collector junctions depletion layers (respectively).

R_B : a parameter

Under saturation conditions δ_E and δ_C are small compared to a_0, and so we can write, from 1:

$$r_B \approx r_B^o + r_B^o \frac{\tilde{\delta_E} + \tilde{\delta_C}}{2a_0} \qquad (5)$$

Where δ_E and δ_C are the alternate components of δ_E and δ_C when alternate small signal voltages are present across the emitter and collector junctions.

For this small signal case, $\tilde{\delta_E}$ and $\tilde{\delta_C}$ are proportional to the negative of the voltages across the respective junctions, so that 2 becomes:

$$r_B = r_B^o - k_E\tilde{v_{EB}} - k_C\tilde{v_{EC}} \qquad (6)$$

where k_E and k_C are positive proportionality constants.

The equivalent circuit of the transistor is then as in Fig. 2, where z_E' and z_C' now include the depletion capacitances of the respective junctions.

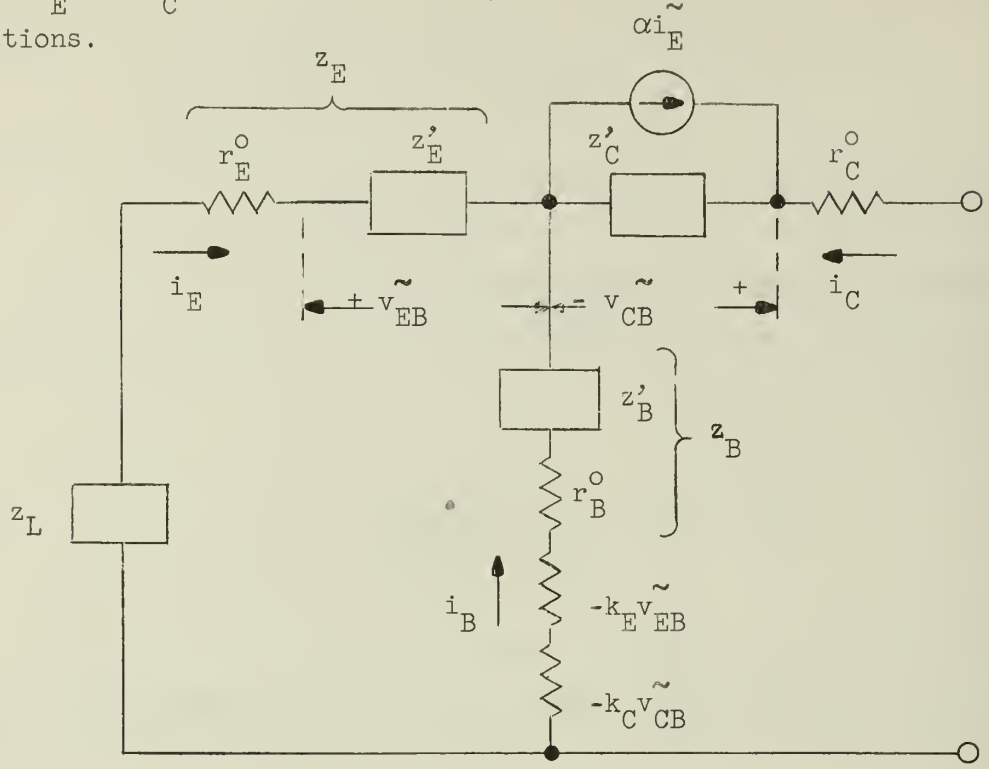

Equivalent Circuit Including Simplified Early Effect

Figure 2. $z_E' = z_E^1 \,||\, C_E$; $z_C' = z_C^1 \,||\, C_C$; $z_B' = z_B^1$

z_E^1, z_C^1 and z_B^1 as given in Part I, where effects of base storage capacitance are already included.

Then we have, with $i_E = \bar{i_E} + \tilde{i_E}$ and $i_C = \bar{i_C} + \tilde{i_C}$, and neglecting quadratic forms (second harmonic components):

$$\tilde{v_{CB}} = (\tilde{i_C} + \tilde{i_E}) z_C'$$

and

$$\tilde{v}_{EB} = \tilde{i}_E z'_E \quad -\tilde{i}_E (z_1 + r_E) - (\tilde{i}_E + \tilde{i}_C) z_B \tag{7}$$

$$+ (\bar{i}_E + \bar{i}_C) [k_C (\tilde{i}_C + \alpha \tilde{i}_E) z'_C + k_E \tilde{i}_E z'_E]$$

So that:

$$\tilde{i}_E [z_L + z_E + z_B - I_B (k_E z'_E + \alpha k_C z'_C)] = -\tilde{i}_C [z_B - I_B k_C z'_C]$$

And hence:

$$G_I = \frac{\tilde{i}_E}{\tilde{i}_C} = \frac{z_B - I_B k_C z'_C}{z_L + z_E + z_B - I_B (k_E z'_E + \alpha k_C z'_C)} \tag{8}$$

4. Expanded Expression for G_I

The parameters of the T equivalent circuit obtained in Part I are repeated below for convenience. We consider only the effects of base storage capacitance since the depletion capacitances are much smaller; also, the circuit configuration indicates that the effects of the latter should be negligible at the frequencies considered and biasing conditions since C_E and C_C are practically short circuited by the small impedances z_E^1 and z_C^1 respectively. In fact, we should consider the modulation of the base storage capacitance by the Early effect by replacing w in the parameter expressions with $w_0 = \frac{\delta_E + \delta_C}{2}$ and take into account the modulation of δ_E and δ_C with $\tilde{v}_E$ and $\tilde{v}_C$ respectively. If the signals are small and the frequencies are low, as they indeed are, this would be a small perturbation on the solution of the time dependent diffusion equation, so it would be an acceptable approximation. This refinement, however, would complicate our solution without any real advantage, since we wish only to show, in a qualitative manner, that the modulation of base width indicates the possibility of inverse current amplification in the case of highly saturated transistors. The simplified model of considering a modulated base resistance instead of all effects of modulated base width is entirely satisfactory for this purpose.

The parameters are:

$$z_E = \frac{\rho_E}{2m} + r_E^o = r_E \quad ; \quad z_B = \frac{m\rho_E}{1 + \tau_p s} + r_B^o$$

$$z_C' \approx z_C^1 = \frac{(\rho_C - \rho_E)m}{1 + \tau_p s} + \frac{\rho_C}{2m} \quad ; \quad \alpha = \frac{2(\rho_C - \rho_E)}{2(\rho_C - \rho_E) - \rho_C \frac{1}{m^2}(1 + \tau_p s)} =$$

$$= \frac{\rho_C - \rho_E}{z_C^1 \frac{1}{m}(1 + \tau_p s)} \qquad (9)$$

Hence:

$$z_C^1 \alpha = \frac{(\rho_C - \rho_E)m}{1 + \tau_p s} \quad , \quad \text{with } m = \frac{L_p}{a} \text{ and } s \text{ was substituted for } jw.$$

Substitution of Eqs. 6 into 5 yields, in the case of $z_L = r_L$:

$$G_I = - \frac{\frac{m\rho_E}{1 + \tau_p s} + r_B^o - I_B k_C \left(\frac{(\rho_C - \rho_E)m}{1 + \tau_p s} + \rho_C \frac{1}{2m}\right)}{r_L + r_E + r_B^o + \frac{m\rho_E}{1 + \tau_p s} - I_B k_E \frac{\rho_E}{2m} - I_B k_C \frac{(\rho_C - \rho_E)m}{1 + \tau_p s}}$$

multiplying both numerator and denominator by $1 + \tau_p s$ and rearranging terms we get:

$$G_I = - \frac{\left\{m[\rho_E - I_B k_C(\rho_C - \rho_E)] + r_B^o - I_B \frac{k_C \rho_C}{2m}\right\} + [r_B^o - I_B \frac{k_C \rho_C}{2m}] \tau_p s}{\left\{m[\rho_E - I_B k_C(\rho_C - \rho_E)] + [r_L + r_E + r_B^o - I_B \frac{k_E \rho_E}{2m}]\right\} + [r_L + r_E + r_B^o} \cdots$$

$$\cdots \frac{}{- I_B \frac{k_E \rho_E}{2m}] \tau_p s} \qquad (10)$$

5. Qualitative Discussion of G_I

(a) Notice first that, if r_L were instead $\frac{1}{C_L s}$, depending on the values of the coefficients, we could have a pair of complex poles on the left half plane and then G_I would have the characteristic of a resonance curve.

(b) With r_L itself, Eq. 10 is of the form:

$$G_I = - \frac{A + B + B\tau_p s}{A + C + C\tau_p s} \tag{11}$$

with A, B and C all functions of saturation level through parameters such as I_B, k_E, k_C, ρ_E, ρ_C and even m; all are real and can be either positive, negative, or zero; they are not independent, really, since geometry of the transistor, doping levels and biasing conditions determine all of them, and from these variables only the biasing conditions can be controlled with a given sample. Hence, given a transistor, there are only two degrees of freedom for the three variables, namely I_E and V_C.

However, we do not have these dependences explicitly in Eq. 7, so we will just assume that A, B and C can assume arbitrary values and see what happens to G_I in each case:

Signals of			Conditions	$\lvert G_I \rvert$	Conditions	$\operatorname{sgn} G_I$
A	B	C				
+	+	+	$\lvert B \rvert > \lvert C \rvert$	> 1		-
			$\lvert B \rvert < \lvert C \rvert$	< 1		-
+	+	-	$\lvert A \rvert < \lvert C \rvert$	> 1		+
			$\lvert A \rvert > \lvert C \rvert$	unstable		?
+	-	+	$\lvert A+B \rvert > \lvert A+C \rvert$	> 1		+
			$\lvert A+B \rvert < \lvert A+C \rvert$	< 1	$\lvert B \rvert < \lvert A \rvert$	-
					$\lvert B \rvert > \lvert A \rvert$	+

UNIVERSITY OF

Signals of			Conditions	$\lvert G_I \rvert$	Conditions	$\operatorname{sgn} G_I$
+	-	-	$\lvert A \rvert < \lvert C \rvert$	$\lvert A+B \rvert > \lvert A+C \rvert > 1$		-
				$\lvert A+B \rvert < \lvert A+C \rvert < 1$	$\lvert A \rvert < \lvert B \rvert$	-
					$\lvert A \rvert > \lvert B \rvert$	+
				$\lvert A \rvert > \lvert C \rvert$ unstable		?
-	+	+	Same conditions and values of			
-	+	-	$\lvert G_I \rvert$ and same values of $\operatorname{sgn} G_I$			
-	-	+	as their negatives			
-	-	-				

So, all combinations would possibly agree with the experimental results, as far as having a gain larger than one. Two more experimental facts narrow down the possibilities: (i) Since no zero of G_I was measured, we assume that $|B| << |C|$; (ii) with a resistive load and at low frequencies the gain is negative. So only two possibilities remain: + - - and - + + combinations, with $|B| << |C|$, $|A| < |C|$, $|A+B| > |A+C|$.

So the expression does imply the possibility of a gain larger than one with the characteristics observed.

It is seen that the situation in which this happens is a very critical one, so that it may or may not occur with a given type of transistor.

Besides magnitude and signal at low frequencies, frequency, response, i.e., effect of z_L is also qualitatively accounted for; low cut-off frequency comes from the fact that $|G_I| > 1 \Rightarrow \frac{A + C}{C\tau_p}$ must be small. The fact that increasing r_L decreases $|G_I|$ is obvious from Eq. 7, in any case. Instability is also accounted for by the possibility of a right half plane pole for some conditions.

We should point out that the measurements of supersaturation inverse gain was by no means exhaustive, and it is possible that, at

different operating points the signal of the gain would be reversed, or the frequency response modified by the inclusion of a zero (possibility of larger values for $|B|$).

6. Quantitative Example

Expression (8) is more suitable than (10) for a quantitative example. The constants k_E and k_C can be obtained from the following relations for the depletion layer width δ:

$$\text{Abrupt junction:} \quad \delta_E = \left(\frac{2\epsilon(-V_E)}{q(n_D - n_A)} \right)^{1/2} \tag{12}$$

$$\text{Graded junction:} \quad \delta_C = \left(\frac{12\epsilon(-V_C)}{q\nu} \right)^{1/3} \tag{13}$$

(Obs: Considering that in the GF-45011 the emitter junction is abrupt and the collector junction is graded).

Where: $V_E = V_{DE} + \bar{v_E} + \tilde{v_E}$, $V_E < 0$

$V_C = V_{DC} + \bar{v_C} + \tilde{v_C}$, $V_C < 0$

V_{DE}, V_{DC} = diffusion voltages across the emitter and collector junctions respectively; in general we have, with respect to the base:

$$V_D = \frac{kT}{q} \ln \left(\frac{p_n^o}{p_p^o} \right) \tag{14}$$

So that $V_D < 0$

ϵ = dielectric constant of the crystal

q = electron charge

n_D, n_A = donor and acceptor concentrations, respectively, at the n-side and p-side of the abrupt junction.

ν = rate of change of impurity concentration across the junction: $n_D(x) - n_A(x) = \nu x$, for a graded junction.

(See Spenke, Electronic Semiconductors, Chapter IV, Sections 9, 10)
So that, if $\delta = \bar{\delta} + \tilde{\delta}$, and if $|\tilde{\delta}| << \bar{\delta}$, we can approximate:

$$\tilde{\delta} = - \frac{d\delta}{d(-V)} \cdot \tilde{v}$$

We have, in each case, then, since $-V = |V|$ in both cases,

$$\delta_e = - \frac{1}{2} \left(\frac{2\epsilon}{q(n_D - n_A)|\bar{V}_E|} \right)^{1/2} \tilde{v}_E \,, \quad \bar{V}_E = V_{DE} + \bar{v}_E \tag{15}$$

$$\tilde{\delta}_c = - \frac{1}{3} \left(\frac{12\epsilon}{q\nu|\bar{V}_C|^2} \right)^{1/3} \tilde{v}_C \,, \quad \bar{V}_C = V_{DC} + \bar{v}_C \tag{16}$$

And since $r_B = r_B^o - k_E \tilde{v}_E - k_C \tilde{v}_C$,

but also $$r_B = r_B^o + r_B^o \frac{1}{2} (\tilde{\delta}_E + \tilde{\delta}_C) \cdot \frac{1}{a_o - \frac{\bar{\delta}_E + \bar{\delta}_C}{2}} \tag{17}$$

we conclude that: With $\dfrac{1}{a_o - \frac{\bar{\delta}_E + \bar{\delta}_C}{2}} = \dfrac{1}{a_o}$,

$$k_E = \frac{r_B^o}{2a_o} \left| \frac{d\delta_E}{dV_E} \right| \quad \text{and} \quad k_C = \frac{r_B^o}{2a_o} \left| \frac{d\delta_C}{dV_C} \right|$$

or:

$$k_E = \frac{r_B^o}{4a_o} \left(\frac{2\epsilon}{q(n_D - n_A)|\bar{V}_E|} \right)^{1/2} \tag{18}$$

$$k_C = \frac{r_B^o}{6a_o} \left(\frac{12\epsilon}{q\nu|\bar{V}_C|^2} \right)^{1/3} \tag{19}$$

At deeper saturation levels, $|V_E^-|$ and $|V_C|$ decrease (especially $|V_C|$, which is large in normal operation) and k_E and k_C become large.

I_B increases from a few μ-amperes to a few m-amperes, i.e., 3 to 4 orders of magnitude.

The values of α have been shown not to decrease too fast.

Let us assume the following values for the parameters appearing in (8) (educated guesses with the aid of Table 6 and the graphs):

$$z_E = r_E = 5.7\Omega \; ; \; z_B = r_B = 40\Omega \; ; \; r_B = 35\Omega \; ; \; z_L = 10\Omega$$

$$z'_E = z^1_E = 5\Omega \quad ; \; z'_C = 100\Omega \quad ; \; \alpha = 0.8 \; ; \; I_B = 5.0 \text{ ma}$$

Some simple calculations derived from available data on Ge diffused junction mesa transistors, indicate the following:

(i) Emitter doping level; $n_A \approx 10^{20} = D$ k_E will be very small

(ii) Collector junction: $\sigma_{Coll} \approx 100 = D$ $n_p \approx 7 \times 10^8$

(iii) Base doping level: $m_D \approx 10^{17} = D$ $n_n \approx 10^{17}$

(iv) Diffusion voltage across collector-base junction: (ii) and (iii) and Eq. 14 yield:

$$V_D = \frac{kT}{q} \ln \frac{n_n}{n_p} \Rightarrow V_D \approx -0.5 \text{ volt},$$

with respect to the base.

(v) When $V_C = -10$ volts, $\delta_C = 4 \times 10^{-4}$ cm; taking $\delta_C^3 = K^3|V_C|$ we obtain:

$$K = \left(\frac{12\epsilon}{q\nu}\right)^{1/3} \approx 2 \times 10^{-4}$$

Assuming that at supersaturation the potential difference across the collector-base junction is small, say $V_C^- = 0.01$ volts, we get for the depletion layer:

$$\delta_C \approx 4 \times 10^{-5} \text{ cm},$$

which is negligible with respect to the

(vi) base width: $a_0 \approx 1.5 \times 10^{-4}$ cm $\approx a_0'$

(vii) From this data we get:

$$k_C = \frac{r_B^C}{6a_0'} \frac{K}{|V_C^-|^{2/3}} = \frac{35 \times 2}{6 \times 1.5 \times (0.01)^{2/3}} \approx 170$$

And substitution of numerical values into (8) yields:

$$G_I = - \frac{40 - 5 \times 10^{-3} \times 170 \times 100}{10 + 5 + 40 - 5 \times 10^{-3} \times 170 \times 100 \times 0.8} = \frac{40 - 85}{55 - 68} = - \frac{45}{13}$$

$$\text{i.e., } G_I \approx -3.5$$

This calculation is meant to be just an example to give us some idea about the orders of magnitude of the numbers involved. An accurate calculation, or even a first order approximation is, at this point, a very difficult task. Even if the exact impurity profile of the GF-45011 (and S-166) were known, we would still have to:

(i) Obtain the expression for G_I in its true three dimensional basis, rather than the simplified one dimensional analysis used here.

(ii) measure, somehow, the "true" values of the T-model equivalent circuit parameters, since the ones measured in this paper are affected by an undetermined error due to the Early effect, as will be shown in the next section; this would be especially difficult to do at the actual amplifying operating points, since there the perturbations introduced by the Early effect become first order phenomena rather than perturbations.

(iii) Calculate k_E, k_C and $\bar{\tau}_p$ as accurately as possible, which could be a fairly difficult task, since the first two quantities depend very critically on the voltages across the junctions, and these are not constant and difficult to determine accurately, and the latter quantity is "some" average value of τ_p, which, on its turn, depends on the minority carrier distribution throughout the base, a function of position which would be very difficult to find accurately, since it would depend on the (not constant in space) impurity concentration and solution of the resulting non-linear diffusion equation.

So, in this section, we have only used first order approximation, aiming at a result correct in order of magnitude, which, surprisingly enough, came to be correct to a first order approximation.

7. Influence of the Early Effect on the Measurement of Parameter Values

We will consider only a low frequency case. Due to the Early effect, the transistor behaves approximately like the equivalent circuit shown in Fig. 3. Hence, if we assume an equivalent circuit as in Fig. 4, the values we obtain for the parameters must reflect the Early effect. This means that r_{EM}, r_{BM}, r_{CM} and α_M will differ from r_E, r_B, r_C and α by quantities Δr_E, Δr_B, Δr_C and $\Delta\alpha$ which will in fact reflect the (neglected) presence of $\tilde{r}_B$.

We would like to have an idea of how the neglecting of $\tilde{r}_B$ affects the measured values r_{EM}, r_{BM}, r_{CM} and α_M of the "true" parameters r_E, r_B, r_C and α.

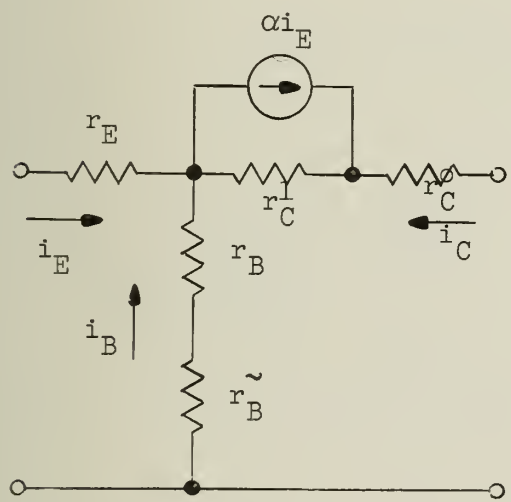

Figure 3. Approximate Equivalent Circuit Considering Early Effect as Represented by $\tilde{r}_B$ only

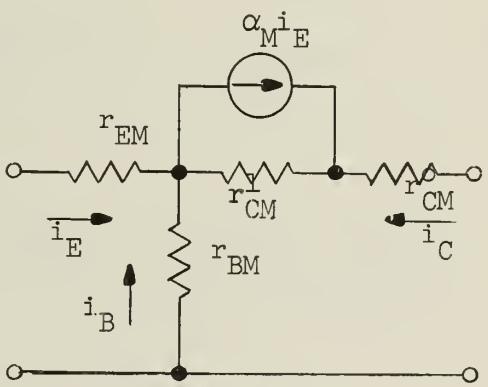

Figure 4. Assumed Equivalent Circuit, with Parameters Modified by Early Effect

To do this, we split the circuit of Fig. 3 into two series connected two-ports, as shown in Fig. 5, and calculate the $\tilde{z}$ parameters of the two-port in the bottom, shown separately in Fig. 6.

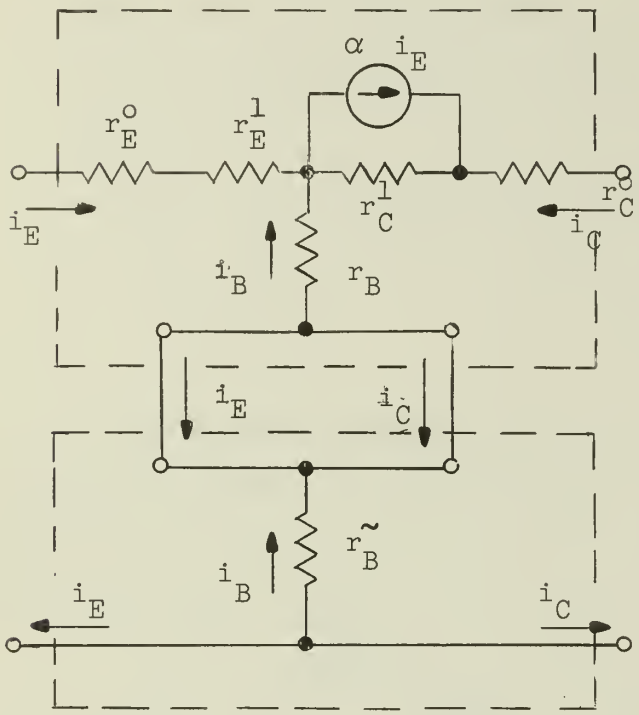

Figure 5. Series Connection of a pair of two-ports equivalent to the circuit of Fig. 3

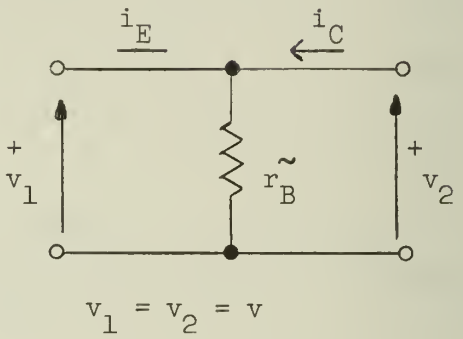

Figure 6. Two-port used to represent Early effect alone

The $\tilde{z}$-parameters here are somewhat artificial, but serve our purpose; they are defined by assuming that i_E and i_C follow separate paths, and obtaining

$$v = \tilde{z}_{11} i_E + \tilde{z}_{12} i_C = \tilde{z}_{21} i_E + \tilde{z}_{22} i_C \qquad (20)$$

We have shown in Section 3 (see Eq. 6) that

$$\tilde{r_B} = -k_E\tilde{v_E} - k_C\tilde{v_C} \; , \tag{21}$$

where $\tilde{v_E}$ and $\tilde{v_C}$ are the alternate voltages respectively across emitter and collector junctions only, not external emitter and collector volatages.
So:

$$\tilde{v_E} = +r_E^{-1}i_E \text{ and } \tilde{v_C} = +r_C^{-1}(i_C + \alpha i_E) \tag{22}$$

And consequently:

$$\tilde{r_B} = -(k_E r_E^{-1} + \alpha k_C r_C^{-1})i_E - k_C r_C^{-1} i_C \tag{23}$$

Since $\tilde{v} = I_B \tilde{r_B}$, where I_B is the absolute value of the base biasing current and second order terms ($i_E\tilde{r_B}$ and $i_C\tilde{r_B}$) have been neglected, we get: (24)

$$\tilde{v} = -I_B(k_E r_E^{-1} + \alpha k_C r_C^{-1})i_E - I_B k_C r_C^{-1} i_C \tag{25}$$

and hence:

$$\begin{aligned} \tilde{z_{11}} &= \tilde{z_{12}} = -I_B(k_E r_E^{-1} + \alpha k_C r_C^{-1}) \\ \tilde{z_{21}} &= \tilde{z_{22}} = -I_B k_C r_C^{-1} \end{aligned} \tag{26}$$

And the z'-parameters of the upper two-port of Fig. 5 are:

$$\begin{aligned} z'_{11} &= r_E + r_B \; ; \; z'_{12} = r_B \\ z'_{21} &= r_B + \alpha r_C^{-1} \; ; \; z'_{22} = r_B + r_C \end{aligned} \tag{27}$$

The z-parameters of the complete circuit are thus:

$$
\left.
\begin{aligned}
z_{11} &= z'_{11} + z''_{11} = r_E + r_B - I_B(k_E r'_E + \alpha k_C r'_C) \\
z_{12} &= z'_{12} + z''_{12} = r_B - I_B(k_E r'_E + \alpha k_C r'_C) \\
z_{21} &= z'_{21} + z''_{21} = r_B + \alpha r'_C - I_B k_C r'_C \\
z_{22} &= z'_{22} + z''_{22} = r_B + r_C - I_B k_C r'_C
\end{aligned}
\right\} \qquad (28)
$$

Since $r_C = r'_C + r^o_C$, and we can assume r^o_C to remain unchanged, in order for the circuit of Fig. 4 to have the same z-parameters as the circuit of Fig. 3, we must have:

$$
\left.
\begin{aligned}
z_{11} &= r_{EM} + r_{BM}\,, \quad z_{12} = r_{BM} \\
z_{21} &= r_{BM} + \alpha r'_{CM}\,, \quad z_{22} = r_{BM} + r_{CM}
\end{aligned}
\right\} \qquad (29)
$$

And then we get successively, by comparing

$$
\left.
\begin{aligned}
r_{EM} &= r_E \\
r_{BM} &= r_B - I_B(k_E r'_E + \alpha k_C r'_C) \\
r'_{CM} &= r'_C + I_B(k_E r'_E - (1 - \alpha) k_C r'_C) \\
r^o_{CM} &= r^o_C \\
\alpha_M &= \cdot \frac{1 + \dfrac{I_B}{\alpha r'_C}\left\{ k_E r'_C - (1 - \alpha) k_C r'_C \right\}}{1 + \dfrac{I_B}{r'_C}\left\{ k_E r'_E - (1 - \alpha) k_C r'_C \right\}}
\end{aligned}
\right\} \qquad (30)
$$

And, in the case where $k_E r_E^1$ is negligible with respect to factors in $k_C r_C^1$ (here we assume $(1 - \alpha)$ is not too small, i.e., under saturation) we have:

$$\left.\begin{aligned} & r_{EM} = r_E \; ; \; r_{BM} = r_B - I_B \; \alpha k_C r_C^1 \\ & r_{CM}^1 = r_C^1 - I_B(1 - \alpha)k_C r_C^1 \; ; \; r_{CM}^o = r_C^o \\ & \alpha_M = \alpha \frac{1 - \frac{1}{\alpha} I_B (1 - \alpha)k_C}{1 - I_B (1 - \alpha)k_C} \end{aligned}\right\} \qquad (31)$$

It should be worth noticing that if the values of k_E and k_C were known to a fair approximation, the "true" parameters r_E, r_B, r_C and α could be calculated from the inverse of Eqs. (30)or (31).

Our aim, however, is to have an idea of how our measured parameters compare with those we use in equations such as (8) or (10), or still, the theoretical formulas as presented in Eqs. (40) to (43) in Part I.

We notice that, in general, the Early effect leaves r_E unchanged, reduces r_B, changes r_C by some positive or negative quantity and changes α by a factor which can be greater or less than one.

And in our particular case, at deep saturation levels, and with negligible factors in $k_E r_E^1$, r_E remains unchanged, r_B and r_C reduced, and, if $\frac{1}{\alpha} I_B (1 - \alpha)k_C < 1$, α is slightly decreased.

The strongest effect is the reduction of r_B; the Early effect is taken care of by an equivalent negative resistor $(-I_B \; \alpha k_C r_C^1)$ in series with r_B, so it is easy to see that the effective base resistance r_{BM} can attain negative values; the effect on r_C is also strong but not so much, since it is seen that k_C would have to reach values close to 1000 in order for the effective collector resistance r_{CM} to be negative: The effect on α is generally negligible.

As an example, assuming the same parameter values of the previous section, we would have measured, according to Eqs. 31

$r_{EM} = 5.7\Omega$ Compare to: $r_E = 5.7\Omega$

$r_{BM} = (40 - 68) = -28\Omega$ $r_B = 40\Omega$

$r'_{CM} = 100 - 17 = 83\Omega$ $r'_C = 100\Omega$

$\alpha_M \approx 0.8 \dfrac{1 - 0.21}{1 - 0.17} = 0.75$ $\alpha = 0.8$

Transistor Specifications

Type: Western Electric GF-45011 (or the equivalent Texas Instruments X-310)
Both satisfy the following specifications:

Parameter	Test Conditions	Initial Specifications	End of Life Specifications
BV_{CB}	$I_E = 0$ $I_C = -100$ μAdc	$\geq$ -30 Vdc	$\geq$ -25 Vdc at -500 μADc
I_{CBO}	$I_E = 0$ $V_{CB} = -20$ Vdc	$\leq$ -5.0 μAdc	$\leq$ -10 μAdc at -20 Vdc
$DC(1 - \alpha)$	$I_E = 10$ ma DC $V_{CB} = -4$ Vdc	$\leq$ .04	$\leq$ .06 at 10 ma DC -4 Vdc
V_{EB}	$I_E = 10$ ma DC $V_{CB} = -4$ Vdc	.30 - .45 Vdc	.30 - .50 Vdc at 10 ma DC -4Vdc
BV_{EB}	$I_E = -100$ μAdc $V_{CB} = 0$	$\geq$ -4.5 Vdc	$\geq$ -4.1 Vdc at -500 μAdc
C_D	$I_E = 0$ $V_{CB} = -10$ Vdc	$\leq$ 2.0 μf	same
h_{fe}	$I_E = 10$ ma DC $V_{CB} = -10$ Vdc f = 100 Mc/sec	$\geq$ 8 db	same
r'_b	$I_E = 10$ ma DC $V_{CB} = -10$ Vdc f = 250 MC/sec	$\leq$ 150 Ω $\geq$ 100 Ω	same
ρ	25°C ambient	$\geq$ 200 mw	same

Where:

BV_{CB} = base-collector breakdown voltage

I_{CBO} = "open-emitter" collector current

$DC(1 - \alpha) = (1 - \alpha)$ for DC conditions i.e., I_C/I_E

V_{EB} = emitter-base forward drop

BV_{EB} = emitter-base breakdown voltage

C_D = collector depletion layer capacitance

h_{fe} = grounded emitter forward current gain, i.e., AC $\frac{\alpha}{1 - \alpha}$ at given frequency in dk.

r'_b = base spread resistance

ρ = collector dissipation

Derating: The maximum collector dissipation allowed to account for temperatures up to $40^{\circ}C$ (ambient) is 120 mw. The maximum emitter-base breakdown voltage actually used in ILLIAC II circuits is 3.2 volts.

BOUND BY
HNM

UNIVERSITY OF ILLINOIS-URBANA
510.84 IL6R v.1 C002 v.111-130(1961)
Some memory elements used in ILLIAC II /
3 0112 088404147